

OXIDATIVE STRESS ALTERS BLOOD-BRAIN BARRIER INTEGRITY

by

Jeffrey James Lochhead

A Dissertation Submitted to the Faculty of the

GRADUATE INTERDISCIPLINARY PROGRAM IN NEUROSCIENCE

In Partial Fulfillment of the Requirements

For the Degree of

DOCTOR OF PHILOSOPHY

In the Graduate College

THE UNIVERSITY OF ARIZONA

2011

THE UNIVERSITY OF ARIZONA

GRADUATE COLLEGE

As members of the Dissertation Committee, we certify that we have read the dissertation

prepared by Jeffrey James Lochhead

entitled Oxidative Stress Alters Blood-Brain Barrier Integrity

and recommend that it be accepted as fulfilling the dissertation requirement for the Degree of Doctor of Philosophy

_____ Date: December 17, 2010

Thomas P. Davis

_____ Date: December 17, 2010

Todd Vanderah

_____ Date: December 17, 2010

Paul St. John

_____ Date: December 17, 2010

Edward French

_____ Date: December 17, 2010

Patrick Ronaldson

Final approval and acceptance of this dissertation is contingent upon the candidate's submission of the final copies of the dissertation to the Graduate College.

I hereby certify that I have read this dissertation prepared under my direction and recommend that it be accepted as fulfilling the dissertation requirement.

_____ Date: December 17, 2010

Dissertation Director: Todd Vanderah

STATEMENT BY AUTHOR

This dissertation has been submitted in partial fulfillment of requirements for an advanced degree at the University of Arizona and is deposited in the University Library to be made available to borrowers under rules of the Library.

Brief quotations from this dissertation are allowable without special permission, provided that accurate acknowledgment of source is made. Requests for permission for extended quotation from or reproduction of this manuscript in whole or in part may be granted by the head of the major department or the Dean of the Graduate College when in his or her judgment the proposed use of the material is in the interests of scholarship. In all other instances, however, permission must be obtained from the author.

SIGNED: Jeffrey James Lochhead

ACKNOWLEDGEMENTS

I would first like to thank my mentor and adviser Dr. Thomas P. Davis for allowing me to do this work in his laboratory. I greatly appreciate his guidance over the years and his willingness to let me work on projects of my choosing. I would also like to thank my PhD committee: Drs. Paul St. John, Patrick Ronaldson, Todd Vanderah, and Edward French for their advice and support.

While in the Davis lab, I have had the opportunity to work with many talented scientists and good people. I would like to thank Dr. Melissa Fleegal-DeMotta for teaching me cell culture and Western blot techniques. I would also like to thank Drs. Richard Egleton, Brian Hawkins, Ken Witt, Scott Ochletree, Tracy Brooks, and Will Staatz for their support.

In addition, I have had the pleasure of working with several other graduate students who made my time in the lab so enjoyable. Thank you to Dr. Sharon Hom, Dr. Melissa Seelbach, Dr. Christopher Campos and Lucy Sanchez-Covarrubias for the laughs and memories I will never forget.

I have also had the pleasure of working with talented undergraduate students over the years. To Carolyn Quigley, Nikki Nametz, Colleen Quigley, Christine Solinsky, Jessica Finch, and Kristin DeMarco, thank you for all the help and fun times over the years.

A special thank you to Dr. Gwen McCaffrey. Your subcellular fractionation expertise was the inspiration and driving force for this dissertation work. Your hard work and kind nature will forever be appreciated.

I would also like to acknowledge my parents, Maggie and Jim Lochhead as well as my extended family and wonderful friends. You have always been nothing but supportive of me. Thank you all.

DEDICATION

I would like to dedicate this work to Antoinette Wisnewski, Anna and Jim Lochhead Sr., and Richard Caniglia. I love and miss you all.

TABLE OF CONTENTS

LIST OF FIGURES.....	8
LIST OF TABLES.....	9
ABSTRACT.....	10
CHAPTER 1: INTRODUCTION TO THE BLOOD-BRAIN BARRIER.....	12
1.1 The Blood-Brain Barrier.....	13
1.2 History of the Blood-Brain Barrier.....	14
1.3 Concept of the Neurovascular Unit.....	18
1.4 Molecular Organization of the Blood-Brain Barrier.....	24
1.5 The Blood-Brain Barrier in Disease States.....	34
CHAPTER 2: OXIDATIVE STRESS AND THE BLOOD-BRAIN BARRIER.....	40
2.1 Chemistry and Physiology of Reactive Oxygen Species.....	41
2.2 Effects of Reactive Oxygen Species on Blood-Brain Barrier Function.....	48
2.3 Objectives and Hypothesis of the Present Study.....	50
CHAPTER 3: ROLE OF REACTIVE OXYGEN SPECIES IN BLOOD-BRAIN BARRIER DISRUPTION DURING HYPOXIA-REOXYGENATION.....	52
3.1 Introduction.....	53
3.2 Experimental Procedures.....	55
3.3 Results.....	62

3.4 Discussion.....	77
CHAPTER 4: ROLE OF REACTIVE OXYGEN SPECIES IN BLOOD-BRAIN BARRIER DISRUPTION DURING PERIPHERAL INFLAMMATORY PAIN.....	84
4.1 Introduction.....	85
4.2 Experimental Procedures.....	87
4.3 Results.....	94
4.4 Discussion.....	103
CHAPTER 5: SUMMARY AND CONCLUSIONS.....	107
REFERENCES.....	113

LIST OF FIGURES

Figure 1.1 Comparison of endothelium in the CNS and the periphery.....	17
Figure 1.2 Cell-cell signaling in the neurovascular unit.....	23
Figure 1.3 Position of conserved cysteines within occludin.....	26
Figure 1.4 Molecular organization of tight junction and adherens junctions at BBB.....	30
Figure 1.5 Schematic of the various mechanisms and routes of transport at the BBB.....	33
Figure 2.1 Mitochondrial ROS and endogenous antioxidant systems.....	47
Figure 3.1 Hypoxia and reoxygenation induces Hif-1 α translocation to the nucleus.....	64
Figure 3.2 Oxidative stress induces expression of heat shock protein 70.....	67
Figure 3.3 Effects of hypoxia and reoxygenation and tempol treatment on BBB permeability.....	70
Figure 3.4 Oxidative stress induces changes in occludin localization.....	72
Figure 3.5 Density gradient fractionation of cerebral microvessels and occludin OD.....	76
Figure 4.1 Effect of carrageenan induced pain and tempol on paw edema and thermal hyperalgesia.....	95
Figure 4.2 Nuclear expression of NF- κ B.....	97
Figure 4.3 Effect of carrageenan induced pain and tempol on BBB permeability.....	99
Figure 4.4 Effect of carrageenan induced pain and tempol on occludin oligomers.....	102

LIST OF TABLES

Table 2.1 Common ROS and their biochemical properties.....	43
Table 3.1 Mander's colocalization coefficients for Hif-1 α and TO-PRO-3.....	65
Table 3.2 Percentage of cerebral microvessels exhibiting punctate staining of occludin.....	73

ABSTRACT

The blood-brain barrier (BBB) is located at the level of the cerebral microvasculature and is critical to maintain central nervous system (CNS) homeostasis. The tight junction (TJ) protein complexes between endothelial cells at the BBB are primarily responsible for limiting paracellular diffusion of substances from the blood to the CNS. The BBB's functional integrity is compromised in a number of disease states which affect the CNS, suggesting BBB dysfunction causes or contributes to many diseases of the CNS. A common component of most of these diseases is oxidative stress. Oxidative stress is associated with hypoxia-reoxygenation (HR) and peripheral inflammatory pain (PIP). Both HR and PIP have been shown to compromise BBB functional integrity. Using *in vivo* rat models of HR and PIP, we examined the role of ROS on BBB permeability as well as the TJ protein occludin using the free radical scavenger tempol. First, we subjected rats to HR with or without pre-treatment with tempol (200 mg/kg). We showed that tempol prevents up-regulation of the cellular stress marker heat shock protein 70 at the BBB during HR. Next we showed tempol reverses HR-mediated BBB permeability increase to ¹⁴C-sucrose, a marker of BBB paracellular permeability. Tempol also attenuated changes in the structure and localization of occludin, suggesting ROS produced during HR alter occludin and lead to disruption of BBB. We then investigated whether ROS production have similar effects on occludin and BBB permeability during PIP by administering 3% λ-carrageenan into the hind paw of

rats. We found tempol attenuated carrageenan-induced increase in paw edema and thermal hyperalgesia. Tempol also attenuated up-regulation of the cellular stress marker NF- κ B in cerebral microvessels. Tempol significantly decreased BBB permeability to 14 C sucrose during PIP. We found PIP reduces disulfide bonds in occludin oligomeric assemblies thought to be important in maintaining the structural integrity of the BBB. Tempol significantly inhibited disulfide bond reduction, suggesting ROS mediate BBB disruption during inflammatory pain by reducing occludin disulfide bonding. Taken together, these findings show the involvement of ROS during HR and PIP contributes to BBB dysfunction by altering the structure of high molecular weight occludin oligomeric assemblies.

CHAPTER 1

INTRODUCTION TO THE BLOOD-BRAIN BARRIER

1.1 The Blood-brain Barrier

The central nervous system (CNS) consists of the brain and spinal cord and is a complex, highly evolved, physiological system responsible for regulating the body's response to internal and external stimuli. The CNS requires a tightly regulated environment in order to efficiently encode and process the vast amounts of information it receives. The brain constitutes only 2% of the total body mass while it consumes 20% of the body's energy. The brain requires a constant supply of blood and is very sensitive to decreases in blood flow because it has no local energy reserve. The total length of capillaries in the human brain is close to 400 miles while the available surface area is 12-18 m² (Abbott et al., 2010).

Precise gradients for ions such as K⁺, Na⁺, Cl⁻, and Ca²⁺ must be properly controlled in order for action potentials to occur. Serum proteins, such as albumin, which are abundant and essential for proper physiological function in the periphery, can be neurotoxic (Hassel et al., 1994). Extracellular levels of neurotransmitters must be properly maintained to avoid disturbances in CNS function. Many substances and their metabolites originating from diet or pharmacological intervention may be harmless to peripheral organ systems, but quite neurotoxic within the CNS.

CNS homeostasis is critical to maintain proper function. In order to prevent concentration fluctuations of various blood-borne substances from adversely affecting the CNS, the blood-brain barrier (BBB) has evolved at the level of the cerebral microvasculature. All areas of the brain possess a BBB except those in direct contact

with the ventricular system. The BBB is a dynamically regulated physical and metabolic barrier which is necessary for proper physiological function of the CNS. The BBB is capable of simultaneously restricting potentially neurotoxic substances while essential ions and nutrients are selectively allowed to cross the endothelium from the blood into the brain. BBB disruption is associated with many diseases such as Alzheimer's disease, Multiple Sclerosis, stroke, diabetes, and HIV encephalitis (HIVE) and HIV-associated dementia (HAD) (Zlokovic, 2008; Toborek et al., 2005; Huber, 2008) and an inability of the BBB to properly function may ultimately cause or contribute to diseases affecting the CNS.

1.2 History of the Blood-Brain Barrier

In the 1880s, German scientist Paul Ehrlich noted that most acidic dyes readily stain tissues outside the CNS, but fail to stain most tissue of the CNS (Ehrlich, 1887). He attributed these observations to the nervous tissue lacking any appreciable chemical affinity for the non-staining dyes. Other investigators noted that intravenous injected (i.v.) bile acids or ferrocyanide induce no central pharmacological effects, but injections directly into the CNS induce strong pharmacological actions (Lewandowsky 1900). These observations suggested a barrier between substances in the blood and the brain and led Lewandowsky to introduce the term "blood-brain barrier." Several years later, Ehrlich's student Edwin Goldmann performed experiments with the acidic dye trypan blue that further elucidated Ehrlich's observations. Goldmann found that trypan blue administered intravenously (i.v.) stained tissue throughout the body, but the brain and

spinal cord remained virtually unstained. When trypan blue was directly injected into the cerebrospinal fluid (CSF), however, the nervous tissue was heavily stained (Goldmann 1909, 1913). This showed the nervous tissue does have a chemical affinity for trypan blue and also suggested a barrier between the CNS and peripheral tissues.

Several lines of evidence suggested a selective permeability of the BBB. Ehrlich observed that a limited number of basic dyes would stain the CNS when administered i.v. In addition, studies with deuterated water as a tracer showed establishment of a rapid equilibrium between water in the blood and CSF. It was also known that the concentrations of certain ions were different in the blood and the CSF (Dobbing, 1961), suggesting a mechanism of selectivity for ions within the CNS. These observations led some to question the existence of a BBB. It would take several decades and the advent of electron microscopy (EM) before the anatomical nature of the BBB was revealed.

Using the tracer horseradish peroxidase and EM, Reese and Karnovsky demonstrated brain endothelium is less permeable to peroxidase than vascular endothelium of the heart or skeletal muscle (Reese and Karnovsky, 1967). They provided evidence that reduced vascular permeability in the brain to peroxidase could be explained primarily by structural differences in the junctions between endothelial cells in the brain. Peroxidase failed to penetrate the intercellular tight junctions which fuse the outer leaflets of adjacent brain endothelial plasma membranes. Vesicles thought to participate in transporting materials from the luminal side to the perivascular space of endothelial cells were also scarce in the brain compared to cardiac and skeletal muscle.

A reduction in transport between the luminal and abluminal sides of the brain endothelium was suggested to contribute to its barrier properties (Reese and Karnovsky, 1967). Later studies by Brightman and Reese showed that peroxidase injected into the brain can diffuse between astrocytic foot processes and the perivascular space (Brightman and Reese, 1969). These observations settled a long-standing debate as to whether the anatomical basis of the BBB is at the level of the astrocytic foot processes that ensheath the perivascular space of the endothelium, the basal lamina, or the endothelium itself. It is currently accepted that the BBB exists at the level of the cerebral microvasculature and is characterized by having few transport vesicles and the presence of intercellular tight junctions and a lack of fenestrations.

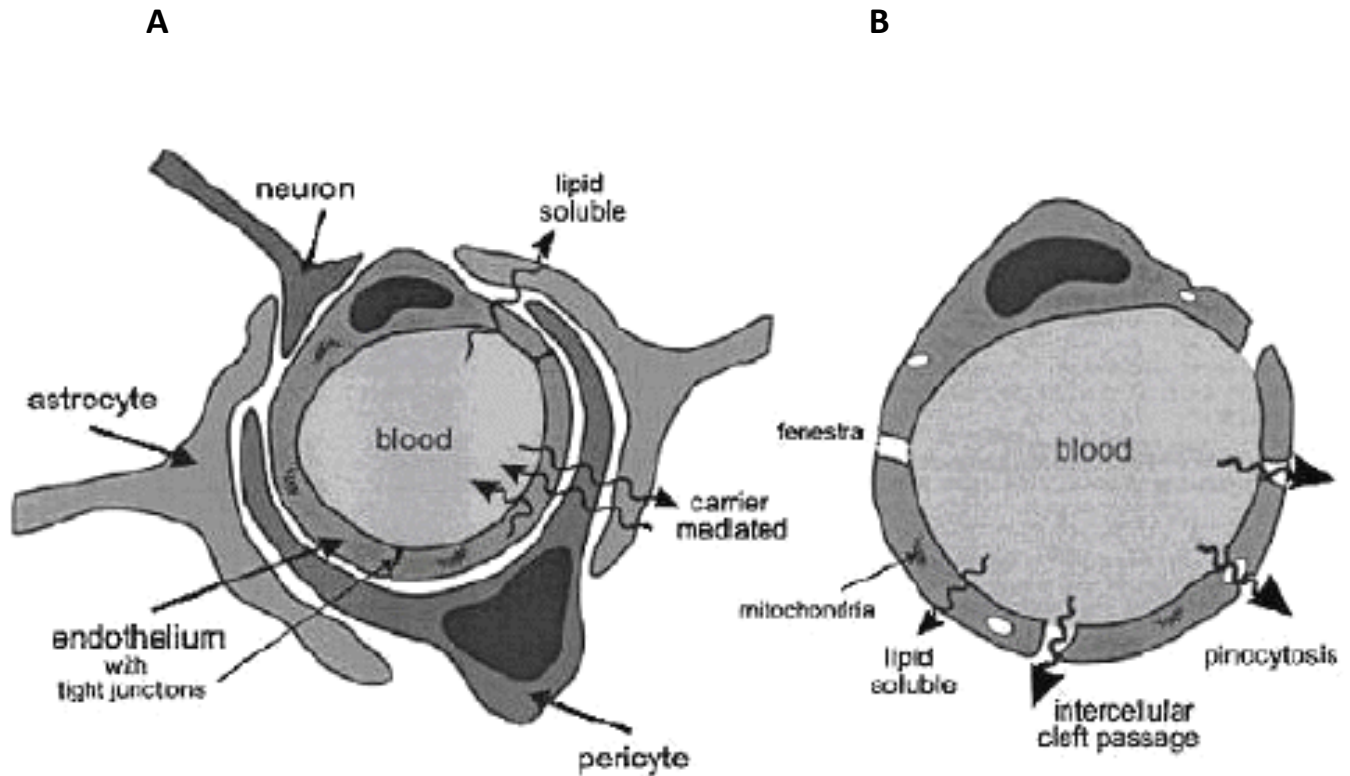


Figure 1.1 Comparison of endothelium in the CNS and the periphery. Endothelial cells in the CNS (A) are sealed to apposing cells by the TJ, which restrict paracellular diffusion of hydrophilic molecules. Brain microvascular endothelial cells are surrounded by pericytes and receive input from astrocytic end feet and neuronal processes. Peripheral endothelial cells (B) lack TJ and have increased rates of pinocytosis, allowing molecules to diffuse intercellularly from the blood. Figure taken from Misra et al., 2003.

1.3 Concept of the Neurovascular Unit

Once it became clear that microvessels in the brain are phenotypically different than microvessels innervating other organs, researchers began to address how brain microvessels acquired their barrier properties. In 1981, Stewart and Wiley conducted experiments investigating the role of the neural tissue environment in differentiating the BBB (Stewart and Wiley, 1981). They transplanted embryonic brain fragments to the coelomic cavity to expose them to non-neural vessels. Additionally, fragments of the embryonic mesoderm were transplanted to the brain where they could be vascularized by neural vessels. It was found that the abdominal vessels acquired structural, functional, and histochemical features of the BBB when vascularizing grafted neural tissue. In contrast, BBB characteristics were absent when brain vessels vascularized grafted mesodermal tissue. These results suggest BBB differentiation is regulated by factors expressed within the neural environment. Over the past several decades, it has become increasingly clear that brain endothelial cells are but one part of a functional unit and are in constant communication with other cell types in the CNS.

The BBB is an essential component of the neurovascular unit (NVU). The NVU consists of brain microvessels which are in close proximity with astrocytic end feet, pericytes, microglia, and neuronal processes. Regulated intercellular signaling in the neurovascular unit is essential for proper neuronal activity to occur. The endothelium is the primary point of contact between the blood and the brain and delivers vital

nutrients to the brain while restricting the passage of neurotoxic substances. Nearly every neuron in the human brain is thought to have its own capillary (Zlokovic, 2008). The brain vasculature locally increases its diameter in response to neuronal firing in order to meet metabolic demand. This vascular contractility is dependent, in part, on pericytes which contain contractile proteins as well as a number of vasoactive mediators (Hamilton et al., 2010).

Pericytes are thought to be of mesodermal origin and migrate into the brain during the latter stages of vascularization (Guillemin and Brew, 2004). Brain capillary pericytes are contained entirely within a basement membrane that they share with the endothelium. Pericytes are typically localized over the tight junction (TJ) regions of the endothelium and they may extend longitudinal cytoplasmic processes to more than one microvessel. In addition to their role in vascular contractility, pericytes also synthesize basement membrane components such as type IV collagen, glycosaminoglycans, and laminin (Fisher, 2008). Pericytes have been shown to regulate BBB-specific gene expression and polarization of astrocyte foot processes ensheathing the vasculature (Armulik et al., 2010). Interestingly, it has also been suggested that pericytes have the ability to act as neural stem cells (Dore-Duffy, 2008).

Neuronal signal conduction involves interactions between neurons and astrocytes while BBB integrity is dependent on signaling between astrocytes and endothelial cells. Within the NVU, astrocytes are located in a position that allows them to both receive neuronal input and communicate intercellularly with the endothelium.

Perivascular astrocyte end feet wrap around endothelial cells and help regulate brain water transport primarily through the expression of aquaporin-4 (Tait et al., 2008). Astrocytes have been shown to induce barrier properties in non-neural endothelial cells *in vivo* (Janzer and Raff, 1987). Additionally, astrocyte-conditioned media has been shown to induce barrier properties by increasing trans-endothelial electrical resistance (TEER) in *in vitro* BBB models (Rubin et al., 1991). A high TEER correlates with reduced BBB permeability, but does not specifically measure paracellular permeability as it may be affected by the opening of ion channels. Astrocytes are also able to regulate the expression and localization of various transport proteins and enzyme systems on the endothelium (Abbott et al., 2006). A number of chemical mediators which promote the BBB phenotype, such as transforming growth factor β (TGF- β), glial derived neurotrophic factor (GDNF), basic fibroblast growth factor (bFGF), and angiopoietin-1 (ANG1), are also secreted by astrocytes. Correct association of endothelial cells and pericytes in tube-like structures *in vitro* is dependent on the presence of astrocytes, suggesting astrocytes are necessary to properly organize the cerebral microvasculature (Ramsauer et al., 2002). Conversely, some studies suggest endothelial cells secrete factors involved in astrocyte growth and differentiation (Estrada et al., 1990; Mi et al., 2001), further underscoring the importance of signaling between astrocytes and endothelial cells.

The cells primarily responsible for innate and adaptive immune responses within the CNS are microglia. Under normal physiological conditions, microglia have a ramified shape and are said to be in the “resting” state. In the resting state, microglia possess

small cellular bodies and long processes which may directly contact nearby endothelial cells and act as local chemical sensors (Han and Suk, 2005). In response to tissue injury or trauma, microglia may become “activated.” Once activated, microglia retract their processes and their cell bodies become enlarged. Activated microglia may secrete inflammatory cytokines and toxic mediators and are often associated with CNS pathology (Zlokovic, 2008). Activated microglia may become “reactive” microglia during an immune response. Reactive microglia are characterized by a spheroid or rod-like morphology, exhibit phagocytic activity, and may act as antigen presenting cells (Nelson et al., 2002). It is unknown what role microglia play in the development and maintenance of the BBB under physiological conditions, but under pathological conditions microglia are thought to contribute to disruption of the BBB.

While proper BBB function is essential for neural transmission, less is known regarding how neurons influence the BBB. One study suggests neurons can induce BBB related enzymes such as Na⁺/K⁺ ATPase and γ -glutamyl transpeptidase (GGTP), which mediates the uptake of neutral amino acids (Tontsch and Bauer, 1991). Further studies will need to be performed to elucidate the exact role that neurons play in the development and maintenance of the BBB.

It has become increasingly clear that all cells of the NVU must work in conjunction with each other in order to maintain brain homeostasis and function. It is difficult to replicate the exact anatomy of the NVU *in vitro*. Endothelial cells are often grown on flat, porous membranes in cell culture, while they form tubular-like structures

in vivo. Co-cultures of brain endothelial cells contain some, but not all, cells present in the NVU and often have TEER values up to one order of magnitude lower than that observed *in vivo*. These considerations make *in vivo* studies of BBB structure and function essential to understanding the physiology and pathophysiology of the BBB.

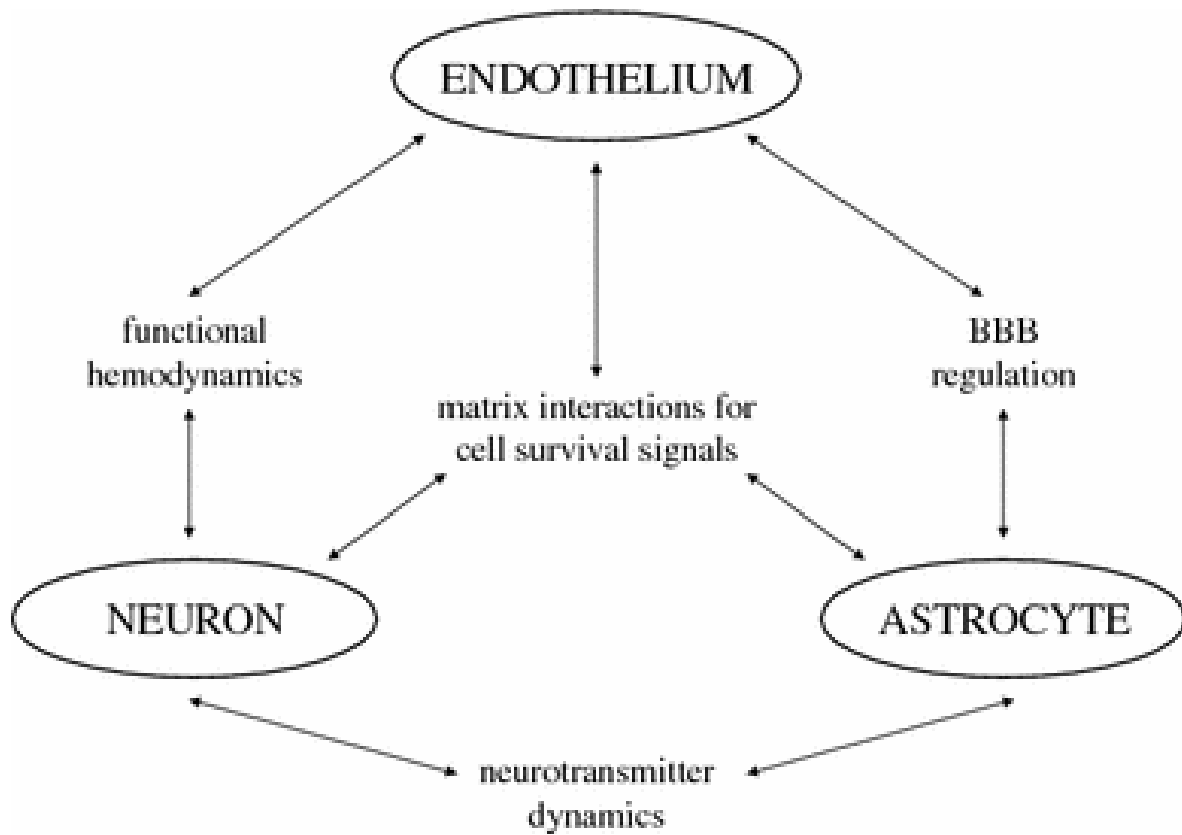


Figure 1.2 Cell-cell signaling in the neurovascular unit. Figure taken from Lok et al., 2007.

1.4 Molecular Organization of the Blood-Brain Barrier

The BBB restricts the passive diffusion of all but small lipophilic molecules <400 Da and dissolved gases such as oxygen (O₂) and carbon dioxide (CO₂) from the blood to the brain. The TEER at the BBB is 1500-2000 Ω·cm² compared to 3-30 Ω·cm² in peripheral endothelium (Crone and Oleson, 1982; Butt et al., 1990). The high TEER at the BBB results in extremely low paracellular permeability and is chiefly due to TJ protein complexes that fuse together the outer leaflets of plasma membranes from adjacent cells. TJ, or *zonula occludens*, are present in polarized epithelial and endothelial cells as well as a variety of specialized epithelial cell types. The major types of proteins constituting the TJ are occludin and the claudins.

Occludin was the first TJ protein discovered in isolated chick livers (Furuse et al., 1993). Human occludin is a 522 amino acid polypeptide with a predicted molecular mass of 59.1 kDa. Occludin contains N- and C-terminal cytoplasmic tails as well as two extracellular loops and a MARVEL (MAL and related proteins for vesicle traffic and membrane link) domain with a four transmembrane-helix architecture. MARVEL domains have previously been associated with proteins present in lipid raft membrane microdomains. It has been shown *in vivo* that occludin exists as high molecular weight oligomers in lipid raft domains at the TJ of the BBB (McCaffrey et al., 2007). Lipid rafts are 10-200 nm structures which are enriched in cholesterol and sphingolipids and are thought to promote protein oligomerization (Jacobson et al., 2007). Proteins targeted to lipid rafts have been associated with various biological processes such as endocytosis,

apoptosis, signal transduction, cell polarization, adhesion, migration, synaptic transmission, and cytoskeletal tethering (Dodelet-Devillers et al., 2009).

A number of *in vitro* studies using truncated and mutant forms of occludin have yielded insight into the roles of specific domains. Deletion of the N-terminus has been shown to decrease the barrier function of TJs (Bamforth et al., 1999). The second extracellular loop is involved in both barrier function and properly localizing occludin at the TJ (Wong and Gumbiner, 1997; Medina et al., 2000). The C-terminus of occludin is important for barrier function and is involved in oligomerization of occludin (Chen et al., 1997) in a redox sensitive manner through disulfide bond formation (Walter et al., 2008). Occludin oligomeric assemblies are held together by disulfide bonds in both hydrophobic and hydrophilic regions of the molecule (McCaffrey et al., 2007) It has also been shown that the C-terminus regulates intracellular trafficking of occludin (Matter et al., 1998) and acts as a site of interaction with regulatory proteins such as the zonula occludens (ZO), which anchor occludin to the actin cytoskeleton (Feldman et al., 2005). There are also serine, threonine, and tyrosine residues on occludin, acting as potential regulatory sites by various kinases and phosphatases. An increase in occludin tyrosine phosphorylation is often associated with an increase in BBB permeability (Takenaga et al., 2009; Haorah et al., 2005) while serine and threonine phosphorylation correlates with occludin localization within the membrane (Andreeva et al., 2001).

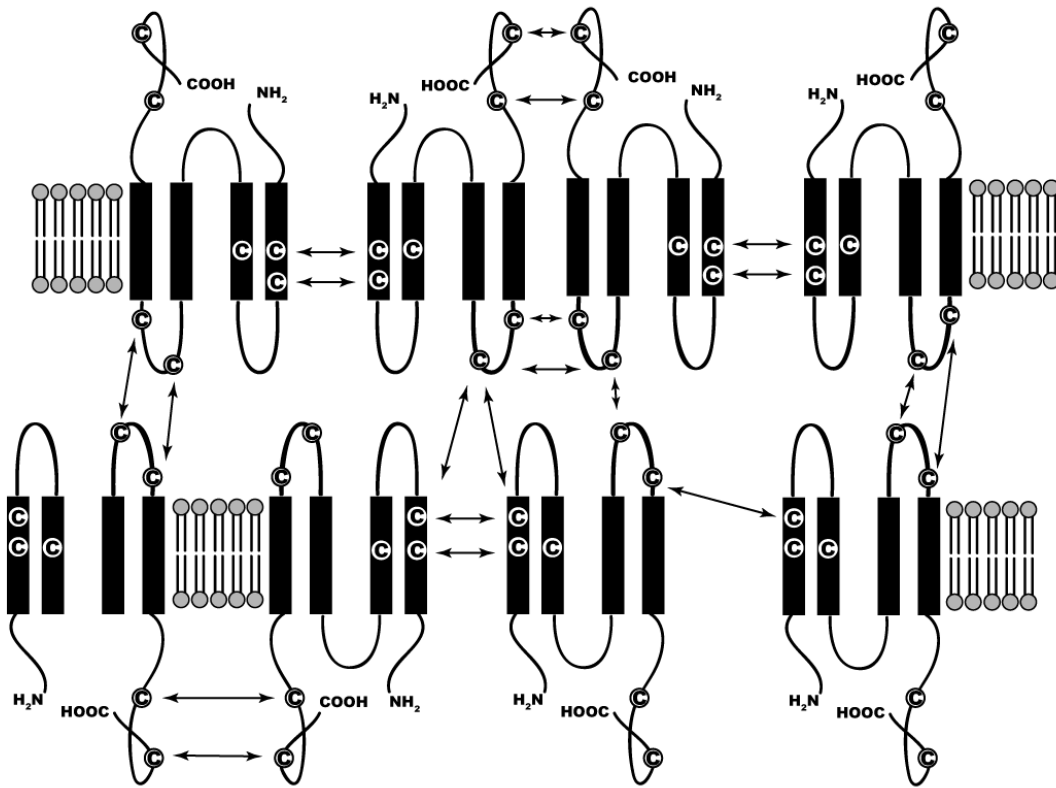


Figure 1.3 – Position of conserved cysteine (C) residues within occludin molecule. Arrows indicate hypothetical disulfide bonds between occludin molecules. Figure courtesy of Dr. Gwen McCaffrey.

In addition to occludin, the claudin family of proteins are expressed prominently at TJs of endothelial and epithelial cells. There are 23 known human claudins. Claudins are 20-27 kDa proteins with four transmembrane regions, two extracellular loops, and N- and C-terminal cytoplasmic tails. All claudins have a PSD-95/Discs-large/ZO-1 (PDZ) binding motif in their C-terminus which allows direct interaction with ZO proteins (Ito et al., 1999). Multiple claudins are expressed in a tissue specific manner by cells which form TJ strands. Specific claudin isoforms have been shown to interact within and between TJ strands (Furuse et al., 1999). Claudin-5 is expressed exclusively by endothelial cells and epithelial cells of the choroid plexus and shows the highest expression levels of any claudin at the BBB (Morita et al., 1999; Lippoldt et al., 2000). Mice deficient in claudin-5 exhibit a size-selective (<800 Da) loosening of the BBB, suggesting claudin-5 is important in maintaining the barrier to small molecules (Nitta et al., 2003).

ZO proteins consist of ZO-1, ZO-2, and ZO-3 and are localized at TJs, adherens junctions (AJ), and/or gap junctions depending on the cell type (Bauer et al., 2010). ZO proteins are members of the family of membrane-associated guanylate kinase (MAGUK) like proteins. They contain three PDZ domains, one SH3 domain, a GUK domain and a proline-rich region (Bauer et al., 2010). ZO proteins function as scaffolding proteins and link occludin and the claudins to the actin cytoskeleton (Furuse et al., 1994; Itoh et al., 1999). ZO-1 is a 220 kDa protein and was the first ZO protein discovered (Stevenson et

al., 1986). ZO-1 knockout is embryonic lethal in mice (Katsuno et al., 2008), but studies in cells lacking ZO-1 show that ZO-1 is involved in targeting claudins and occludin to the TJ as well as establishing barrier properties (Umeda et al., 2004). ZO-2 is a 160 kDa protein which coprecipitates with and has a high sequence homology to ZO-1 (Gumbiner et al., 1991). ZO-2 function at the BBB has been less extensively characterized than ZO-1, but alterations in ZO-2 expression and localization are associated with pathological conditions resulting in BBB disruption (Mark and Davis, 2002; Hom et al., 2007). ZO-3 is a 130 kDa MAGUK protein which also localizes at TJs, but not in endothelial cells (Inoko et al., 2003). In addition to their roles as scaffolding proteins, the ZO proteins contain conserved functional nuclear localization and nuclear export motifs, suggesting they are involved in signal transduction pathways related to gene expression and cell behavior (Bauer et al., 2010).

Junctional adhesion molecule 1 (JAM-1) is a 40 kDa protein which consists of two extracellular immunoglobulin-like (Ig-like) loops, a single transmembrane segment, a short cytoplasmic tail, and homodimerizes (Severson and Parkos, 2009). The C-terminus contains a PDZ binding domain which allows it to interact with TJ accessory proteins such as ZO-1, cingulin, AF-6, and 7H6 (Hawkins and Davis, 2005). Although JAM-1 is not part of the TJ strands, it is thought to be involved in propagating signaling cascades and transendothelial migration of monocytes (Forster, 2008).

Recently discovered as a novel BBB TJ protein is epithelial membrane protein 1 (EMP-1). EMP-1 was found to bind to and colocalize with occludin at the TJ and was

suggested to have a potential role in BBB dysfunction during cerebral ischemia (Bangsow et al., 2008).

Also present at the BBB are the *zonula adherens*, or adherens junctions (AJ). AJ are present in many epithelial and endothelial tissues and are found intermingled with the TJ at the BBB, where they mediate cell-cell adhesion by linking membrane and cytoskeletal components at discrete contact regions. The cadherins are type I, single-pass transmembrane glycoproteins which mediate Ca^{2+} -dependent intercellular adhesion at the TJ (Leckband et al., 2000). The cadherin ectodomain participates in homophilic interactions with cadherin molecules on adjacent cells while the cytoplasmic domain is involved in structural and signaling activities required for adhesion (Niessen and Gottardi, 2008). α -catenin is a vinculin homologue which mediates cadherin's interactions with the actin cytoskeleton (Vasioukhin et al., 2000) while β -catenin stabilizes the core adhesive complex at the cell surface (Huelsken et al., 2000). AJ can also be linked to actin through the nectin/AF-6. AF-6 binds to actin and contains a PDZ binding domain responsible for binding nectin, which contains a C-terminus PDZ binding motif (Niessen and Gottardi, 2008). The role of AJ in regulating BBB permeability has not been extensively studied, but it has been shown that a reduction in VE-cadherin and β -catenin via caveolin siRNA correlates with an increase in paracellular permeability in brain microvascular endothelial cells (Song et al., 2007).

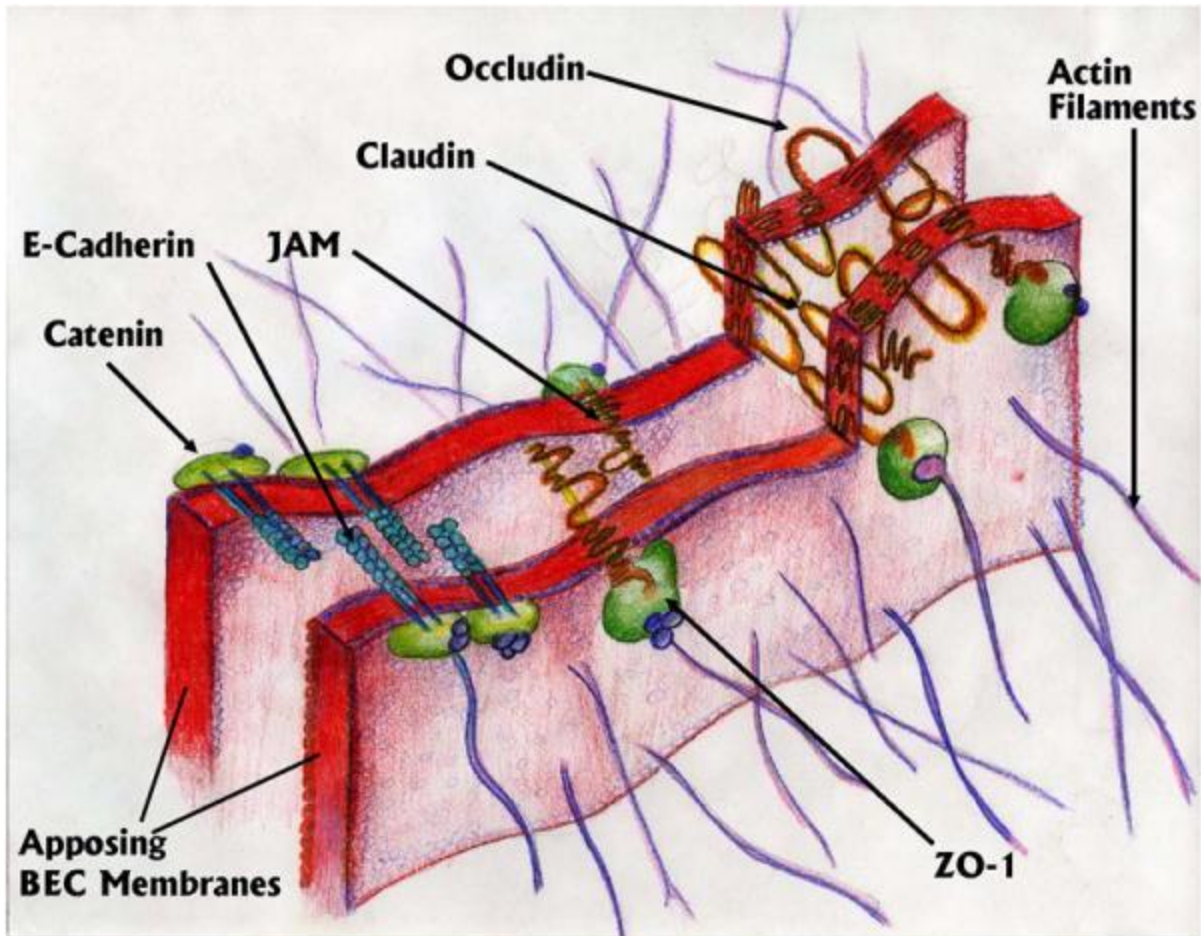


Figure 1.4 – Molecular organization of tight junction and adherens junction proteins at the BBB. Figure taken from Carvey et al., 2009.

While the TJs at the BBB greatly restrict paracellular diffusion of many substances from the blood, many lipophilic molecules can enter the brain by passively diffusing across the endothelial cell membranes. In order to prevent lipophilic xenobiotics from entering the brain where they potentially could exhibit neurotoxicity, the BBB expresses high levels of ATP-binding cassette (ABC) transporters which are able to pump substrates against their concentration gradients utilizing ATP as energy. These transport proteins also control the intake and efflux of many endogenous substances. The most extensively studied ABC transporter at the BBB is ABCB1 or P-glycoprotein (Pgp). Pgp is expressed both lumenally and ablumenally at the BBB, although at much higher levels on the luminal side (Bendayan et al., 2006). Substrates for Pgp include organic cations and weak organic bases with hydrophobic regions, some polypeptides, and an estimated half of all commonly prescribed drugs (Miller, 2010). Also located on the luminal side of the BBB is the multi-drug resistant proteins Mrp-1, Mrp-2, Mrp-4, and Mrp-5 (Ronaldson et al., 2007). Mrp-1 and Mrp-2 efflux hydrophobic organic anions and HIV-protease inhibitors while MRP-4 and MRP-5 efflux cyclic nucleotides and derivatives as well as some organic anions and weak organic acids (Miller, 2010). Breast cancer related protein (BCRP) is also located lumenally and effluxes organic cations and weak organic bases with hydrophobic regions as well as some anionic drugs (Nicolazzo and Katneni, 2009). The BBB also expresses the organic ion transporters Oatp1a4, Oatp1a5, and Oat3 (Ronaldson et al., 2010; Miller, 2010). Oatp1a5 and Oat3 are only expressed ablumenally while Oatp1a4 is expressed on both sides of the BBB. While the

ABC transporters keep potentially toxic substances out of the CNS, they also present a major obstacle to delivering therapeutics to treat CNS disorders.

In addition to the ABC transporters which are able to pump substrates across the membrane, there are also a number of enzymes highly expressed at the BBB plasma membrane which provide a metabolic barrier to detoxify endogenous and exogenous molecules that would otherwise cross the BBB. These include cytochrome P450, aminopeptidases, endopeptidases, and cholinesterase among others (Dauchy et al., 2008; Zlokovic, 2008).

In order to deliver essential nutrients to the brain from the blood that would not normally cross the BBB, a number of transporters are expressed at the luminal surface of the BBB to import these substances. These include transporters and/or receptors for glucose, amino acids, monocarboxylic acids, nucleosides, purines, amines, vitamins, ions, and peptides and proteins such as insulin, leptin, and transferrin (Zlokovic, 2008).

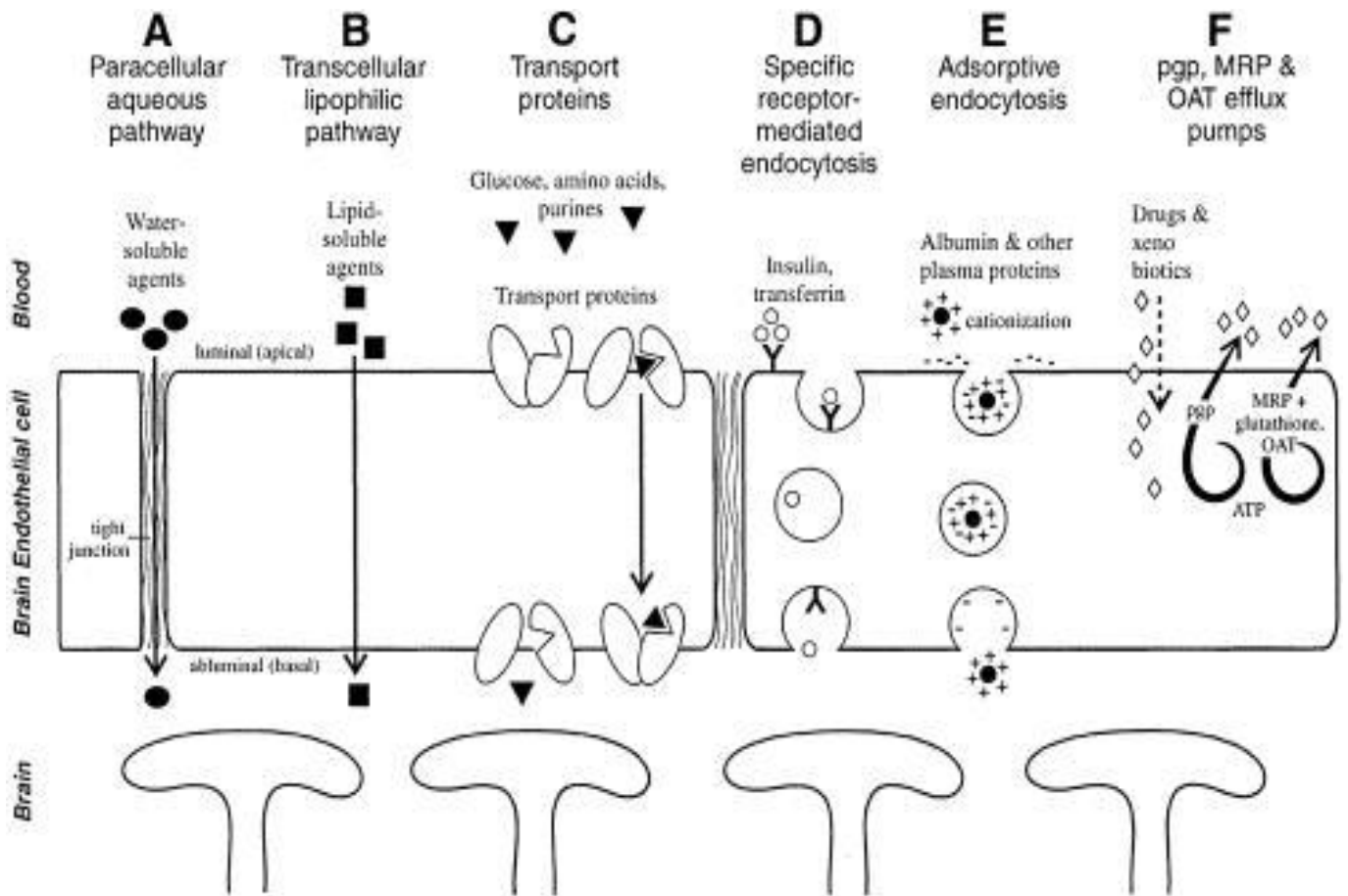


Figure 1.5 – Schematic of the various mechanisms and routes of transport at the BBB.
Figure taken from Neuwelt, 2004.

1.5 The Blood-Brain Barrier in Disease States

The functional integrity of the BBB is compromised in several diseases affecting the CNS. It is often difficult to ascertain whether BBB disruption is the cause, the consequence, or a contributor to disease pathogenesis, but studies utilizing animal models of disease is helping to clarify the BBB's role in the etiology of neurological disease states.

Stroke is a reduction in cerebral blood flow to a region of the brain in association with a vascular injury. Strokes can be either hemorrhagic (approximately 15% of cases) or ischemic (approximately 85% of cases) in origin. Hemorrhagic strokes result from vascular rupture, while ischemic stroke is characterized by an insufficient perfusion to a part of the brain resulting from occlusion or stenosis of a cerebral vessel. Reperfusion following ischemia is associated with a biphasic increase in BBB permeability (Sandoval and Witt, 2008). Increased BBB permeability during ischemia-reperfusion (IR) may lead to potentially neurotoxic solutes entering the brain from the blood as well as vasogenic edema, where increasing paracellular permeability to blood solutes allows fluid to move from intravascular to extravascular spaces. Edema is one of the primary causes of neurological deficits and a leading cause of death following stroke (Sandoval and Witt, 2008). It has been shown that matrix metalloproteinases (MMPs) disrupt the BBB by degrading occludin and claudin-5 as well as basal lamina proteins, such as fibronectin, laminin, and heparan sulfate during the reperfusion phase in animal models of stroke (Rosenberg and Yang, 2007). During experimental stroke, the TJ-associated protein ZO-2

is decreased and the Na⁺/K⁺ ion exchanger NHE-1 is increased, which also may contribute to vasogenic edema (Hom et al., 2007).

A central component of ischemic stroke is hypoxia. A number of studies both in vivo and in vitro have linked hypoxia and/or reoxygenation to an increase in BBB permeability (Sandoval and Witt, 2008). The TJ proteins claudin-5, occludin, ZO-1, and ZO-2 show alterations in expression and/or localization due to hypoxic treatment (Mark and Davis, 2002; Fischer et al., 2002; Brown and Davis, 2005; Koto et al., 2007). Occludin oligomeric assemblies at the TJ of the BBB are also altered by hypoxia and reoxygenation stress (McCaffrey et al., 2009). Hypoxia/aglycemia decreases the AJ protein E-cadherin (Abbruscato and Davis, 1999). The cytoskeletal protein actin also shows rearrangements during hypoxia in brain endothelial cells (Abbruscato and Davis, 1999; Brown and Davis, 2005; Plateel et al., 1995). A number of mediators are thought to be involved in BBB disruption due to hypoxia or reoxygenation. These include interleukin-1 β (Yamagata et al., 2004), protein kinase c (Fleegal et al., 2005; Willis et al., 2010), tissue plasminogen activator (Hiu et al., 2008), nitric oxide (Mark and Davis, 2004), the myosin light chain kinase (Kuhlmann et al., 2007), vascular endothelial growth factor (Schoch et al., 2002), the NMDA receptor (Giese et al., 1995), oxidative stress (Giese et al., 1995; Kimura et al., 2002), MMP-2, MMP-9, MMP-13 (Chen et al., 2009; Lu et al., 2009), and changes in intracellular calcium (Kimura et al., 2000; Brown et al., 2004).

Alzheimer's disease (AD) is the leading cause of dementia and is characterized

pathologically by the presence of insoluble senile plaques and neurofibrillary tangles. The senile plaques are comprised primarily by aggregation of the amyloid β ($A\beta$) protein and accumulate in the neuropil as well as around and inside the cerebral capillaries. According to the amyloid hypothesis, AD is caused by the accumulation of $A\beta$ in the brain due to an imbalance between its production and clearance (Hardy and Selkoe, 2002). The BBB is thought to play a critical role in the maintenance of $A\beta$ levels within the CNS (Bell and Zlokovic, 2009). The low density lipoprotein receptor related protein-1 (LRP-1) expressed on the abluminal side of the BBB has been shown to mediate clearance of $A\beta$ from the brain to the blood (Shibata et al., 2000; Deane et al., 2004) and is down-regulated in AD (Donahue et al., 2006). $A\beta$ is also a substrate for Pgp. At the BBB, Pgp is thought to efflux $A\beta$ from the central nervous system to the blood as well as limit entry of $A\beta$ from the blood to the brain (Ohtsuki et al., 2010). Pgp expression is inversely correlated with $A\beta$ deposition in non-demented elderly humans (Vogelgesang et al., 2002). BCRP expressed at the luminal surface of the BBB has also been shown to limit entry of $A\beta$ from the blood to the brain and BCRP is up-regulated in AD (Xiong et al., 2009). The receptor for advanced glycation end products (RAGE) is also expressed on the luminal surface of the BBB where it can bind and transcytose $A\beta$ from the blood into the CNS (Mackic et al., 1998; Deane et al., 2003). RAGE expression at the BBB is increased in AD (Donahue et al., 2006). $A\beta$ in complex with IgG can also be effluxed from the brain to the blood via the neonatal Fc receptor, which has implications for $A\beta$ immunization therapy (Deane et al., 2005). In addition to its ability to dynamically

regulate A β levels through transport proteins and efflux pumps, the BBB has been shown to be more permeable to plasma proteins in AD patients, suggesting that barrier properties are compromised in AD (Bowman et al., 2007). In a mouse model of AD, an increase in BBB permeability is observed prior to senile plaque formation, suggesting BBB disruption contributes to the pathogenesis of AD (Ujiie et al., 2003).

Multiple sclerosis (MS) is a demyelinating disease which affects the brain or spinal cord and is caused by a combination of autoimmune, genetic, and environmental factors. It has been shown using magnetic resonance imaging (MRI) that BBB disruption precedes symptoms and other pathological lesions in MS (Kermode et al., 1990).

Immunostaining for ZO-1 and occludin at the BBB show abnormal, discontinuous localization in MS (Plumb et al., 2002). The expression of chemokines on endothelial cells at the BBB as well as an increase in MMP activity allows leukocytes to enter the CNS from the blood and release proinflammatory mediators which contribute to the autoimmune response associated with MS (Kurzepa et al., 2005; Holman et al., 2010). BBB disruption is thought to play a central role in the pathogenesis of MS through a decrease in barrier properties and an increase in leukocyte extravasation.

Individuals infected with human immunodeficiency virus (HIV) often develop HIV-related encephalitis (HIVE) or HIV-associated dementia (HAD). Before treatment of HIV with highly active retroviral therapy (HAART), HIVE occurred in approximately one-third of infected patients and HAD affected 15-20% of patients with late stage acquired immunodeficiency syndrome (AIDS). Although HAART has decreased the rate of HAD,

CNS complications may still occur in individuals without access to HAART, individuals who have developed resistance to HAART, or cases of inadequate biological or therapeutic control of viral reservoirs within the brain (Torborek et al., 2005). BBB dysfunction is observed in HIV patients (Petito and Cash, 1992). Histological analysis of occludin and ZO-1 showed a loss of immunoreactivity and a fragmented pattern in patients who died of HIVE (Dallasta et al., 1999) while a loss of ZO-1 immunoreactivity is highly correlated with monocyte infiltration and the degree of dementia in patients with HAD (Boven et al., 2000). It is thought that HIV gains entry into the brain when HIV-infected CD4+ T-lymphocytes and/or circulating monocytes enter through breaches in the BBB (Liu et al., 2000). HIV itself can also cause BBB perturbations. The glycoprotein viral coat of HIV gp120 as well as the Nef protein can increase BBB permeability (Annunziata et al., 1998; Sporer et al., 2000). The HIV Tat protein can also increase BBB permeability in vivo (Arese et al., 2001) and alters the distribution and/or expression of claudin-1, claudin-5, and ZO-2 in brain endothelial cells (Torborek et al., 2005). It is generally accepted that BBB compromise is a key event in HIV entry into the brain and subsequent CNS complications.

A common feature of diseases in which BBB dysfunction has been well characterized is inflammation. Interestingly, inflammatory pain induced outside the CNS by injection of λ -carrageenan or complete Freund's adjuvant into the hind paw of rats can cause increased BBB permeability (Huber et al., 2001). The permeability increase is biphasic in nature and involves changes in expression of the TJ proteins occludin,

claudin-5, JAM-1, and ZO-1 (Huber et al., 2002; Brooks et al., 2005; Brooks et al., 2006). Occludin oligomeric assemblies are also altered 3 hours following hind paw injection of λ -carrageenan (McCaffrey et al., 2008). The permeability changes are attenuated when the cyclooxygenase (COX) inhibitor diclofenac is administered peripherally or when the local anesthetic bupivacaine is administered perineural (Brooks et al., 2008; Campos et al., 2008). These observations suggest both peripheral inflammation as well as nociceptive input can mediate BBB disruption during inflammatory pain. The inflammatory mediator TGF- β has also recently been identified to have a central role in BBB disruption during inflammatory pain (Ronaldson et al., 2009).

The past several decades of research involving BBB dysfunction in various disease states have demonstrated that the BBB is a dynamic structure whose impairment may contribute to disorders of the CNS. A common mechanism linking diseases such as stroke, AD, MS, HIVE and HAD, and inflammatory pain is oxidative stress. The origin of oxidative stress as well as its impact on BBB function will be covered in chapter 2.

CHAPTER 2

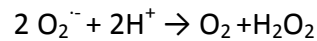
OXIDATIVE STRESS AND THE BLOOD-BRAIN BARRIER

2.1 Chemistry and Physiology of Reactive Oxygen Species

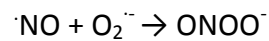
Free radicals are atoms or molecules which contain one or more unpaired electrons. They may be charged or neutral. Most free radicals are unstable due to the unpaired electron and this instability causes them to be highly reactive. The superoxide anion ($O_2^{\cdot -}$) was discovered in the 1930s by Linus Pauling (Pauling, 1979), but free radicals were of little interest to biologists until 1969 when McCord and Fridovich discovered the enzyme superoxide dismutase (SOD) (McCord and Fridovich, 1969). Free radicals, along with other chemically reactive molecules containing oxygen, are collectively referred to as reactive oxygen species (ROS). ROS include free radicals as well as non-radicals such as hydrogen peroxide (H_2O_2) and singlet oxygen which is the electronically excited state of oxygen.

ROS can come from environmental sources such as radiation, cigarette smoke, industrial contaminants, air pollutants, ozone, drugs and alcohol, infection, and foods containing peroxides, aldehydes, oxidized fatty acids, and transition metals (Kohen and Nyska, 2002). They are also produced during reoxygenation/reperfusion (Li and Jackson, 2002) and during every inflammatory response, independently of the causative agent (Di Virgilio, 2004). The major endogenous source of ROS is the mitochondria (Kowaltowski et al., 2009). Approximately 2% of the molecular oxygen reduced in the electron transport chain is converted to the free radical superoxide ($O_2^{\cdot -}$) as a byproduct of respiration. The major sites of $O_2^{\cdot -}$ production within the mitochondria are Complex I and Complex III. $O_2^{\cdot -}$ shows intermediate reactivity relative to other ROS and may act as

an oxidizer or a reductant depending on the molecule it reacts with. $O_2^{\cdot-}$ is detoxified by the antioxidant enzyme SOD according to the following reaction (Forman et al., 2010):



There are three types of SOD. CuZnSOD is produced in the cytoplasm, MnSOD is produced in the mitochondria and extracellular ECSOD is secreted. $O_2^{\cdot-}$ which is not metabolized can react with endogenous NO to form the highly reactive peroxynitrite ($ONOO^{\cdot-}$) according to the following reaction (Li and Jackson, 2002):



Peroxynitrite can oxidize tyrosine residues on proteins to form nitrotyrosine or it may react with bicarbonate to form the carbonate radical ($CO_3^{\cdot-}$) (Medinas et al., 2007).

Although NO is classified by many to be a ROS or reactive nitrogen specie, it is not very reactive itself and its damaging effects are thought to be mediated primarily by the formation of peroxynitrite.

The hydrogen peroxide produced by SOD is membrane permeable is removed by the antioxidant enzymes catalase, glutathione peroxidase, and thioredoxin peroxidase (Kowaltowski et al., 2009). H_2O_2 which is not metabolized can participate in the Fenton reaction with Fe^{3+} or Cu^{2+} to form the hydroxyl radical ($\cdot OH$) which is a potent oxidant that reacts with nearly all biomolecules with a near diffusion limited rate constant (Forman et al., 2010). Table 2.1 summarizes common ROS and their reactive properties.

Table 2.1 Common ROS and their Biochemical Properties

Singlet oxygen	Electronically excited state of oxygen, following UV or other irradiation; reacts with a number of biological molecules, including membrane lipids to initiate peroxidation.
Superoxide	Mild oxidant and reductant with limited biological activity; releases Fe(II) from some iron complexes and iron-sulfur proteins, enabling hydroxyl radical production by the Fenton reaction; has limited membrane permeability.
Hydrogen Peroxide	Oxidizing agent; reacts slowly with reducing agents such as thiols; reacts with reduced iron and copper salts to generate hydroxyl radicals; reacts with heme proteins and peroxidases to initiate radical reactions and lipid peroxidation; membrane permeable.
Hydroxyl radical	Extremely reactive with most biological molecules; causes modification of DNA (with base modification and strand breaks), protein damage and enzyme inactivation, lipid peroxidation, through radical mechanisms; very short range of action
Peroxynitrite	Unstable short lived strong oxidant with properties similar to hydroxyl radical; hydroxylates and nitrates aromatic compounds; reacts rapidly with thiols; breaks down to nitrate; interacts with bicarbonate to alter reactivity.

Table modified from Bergamini et al., 2004

Oxidative stress is the term coined to describe a situation in which ROS production in an organism exceeds the organism's ability to detoxify the ROS. Oxidative stress results in a disruption of redox signaling as well as damage to important macromolecules such as proteins, lipids, and nucleic acids. Free radicals can oxidize double bonds of polyunsaturated lipids, promote strand breaks in DNA, and modify proteins leading to loss of function and/or activation of apoptotic pathways (Laranjinha, 2009). Although known for their prominent role in the pathogenesis of many diseases,

ROS also may act as signaling molecules in a number of different pathways (Forman et al., 2010). At high concentrations, ROS have damaging effects, but at low concentrations ROS may stimulate cell proliferation (Bergamini et al., 2004).

While the mitochondria are the major endogenous source of ROS production, there are various enzymes which produce ROS to act as signaling molecules or kill infectious microorganisms. Enzymes which directly produce ROS include the NADPH oxidase complex and xanthine dehydrogenase/oxidase (XOD). NADPH oxidase is expressed in various cell types during the inflammatory response to produce ROS in response to invading microorganisms in a coordinated process known as the “respiratory” or “oxidative” burst (Laranjinha 2009). NADPH oxidase is a heterodimer consisting of the gp91^{phox} and p22^{phox} (phox stands for phagocyte oxidase) protein subunits. This transmembrane enzyme complex reduces O₂ to O₂^{•-} with NADPH as the one electron donor (Thannickal and Fanburg, 2000). While the ROS produced during the respiratory burst effectively kill microorganisms, they can also indiscriminately react with and damage the molecules in the host. XOD is not normally found under physiological conditions but is formed from xanthine dehydrogenase during hypoxic conditions and is able to generate both O₂^{•-} and H₂O₂ (McKelvey et al., 1988). COX produces free radicals during the synthesis of prostanoids from arachidonic acid and COX-2 is up-regulated during inflammation (Jiang et al., 2004). The cytochrome *P*-450 and *b*₅ enzyme families are also able to oxidize unsaturated fatty acids and some xenobiotics to produce O₂^{•-} and/or H₂O₂ (Thannickal and Fanburg, 2000). Small molecules

such as dopamine and epinephrine may also be autooxidized to produce ROS, usually $O_2^{\cdot -}$ (Thannickal and Fanburg, 2000).

ROS are also often produced in response to ligand-receptor interactions. For example, cultured endothelial cells release $O_2^{\cdot -}$ in response to the cytokines interleukin-1 (IL-1) and interferon gamma (IFN- γ) (Matsubara and Ziff, 1986). IL-1 and Tumor necrosis factor-alpha (TNF- α) cause human fibroblasts to release ROS (Meier et al., 1989). In addition to ROS production following cytokine-receptor binding, ligand binding to various receptor tyrosine kinases (RTKs), receptor serine/threonine kinases, ion channel-linked receptors, and G-protein coupled receptors (GPCRs) is also associated with an increase in ROS (Thannickal and Fanburg, 2000). Oxidative stress can also activate a number of redox-sensitive transcription factors such as nuclear factor kappa B (NF- κ B), activator protein-1 (AP-1), NF-E2 related factor-2 (Nrf2), Cyclic AMP responsive element binding protein (CREB), and p53 which regulate the expression of genes involved in antioxidant defenses as well as cytokines and chemokines (Laranjinha, 2009). This demonstrates the cell's ability to adapt to conditions of elevated oxidative stress.

To combat cellular damage from excessive ROS production, cells express antioxidant enzymes such SOD, catalase, glutathione peroxidase, periredoxins, and the thioredoxin system. Genes coding for these enzymes contain an antioxidant response element (ARE) located in the upstream promoter region which Nrf2 binds to (Lehner et al., 2010). A number of low molecular weight antioxidants are also produced endogenously or acquired through dietary means. These include endogenously

produced glutathione and dietary sources such as uric acid, melatonin, folic acid, carotenoids, Ω -3 fatty acids, coenzyme Q-10, bioflavonoids, and vitamins A, C, E, B1, B2, B6, B12 (Surh et al., 2005; Lehner et al., 2010). The chemistry and physiology of ROS is complex and the pathways primarily responsible for generating mitochondrial ROS and the antioxidant enzymes they react with are summarized in Figure 2.1.

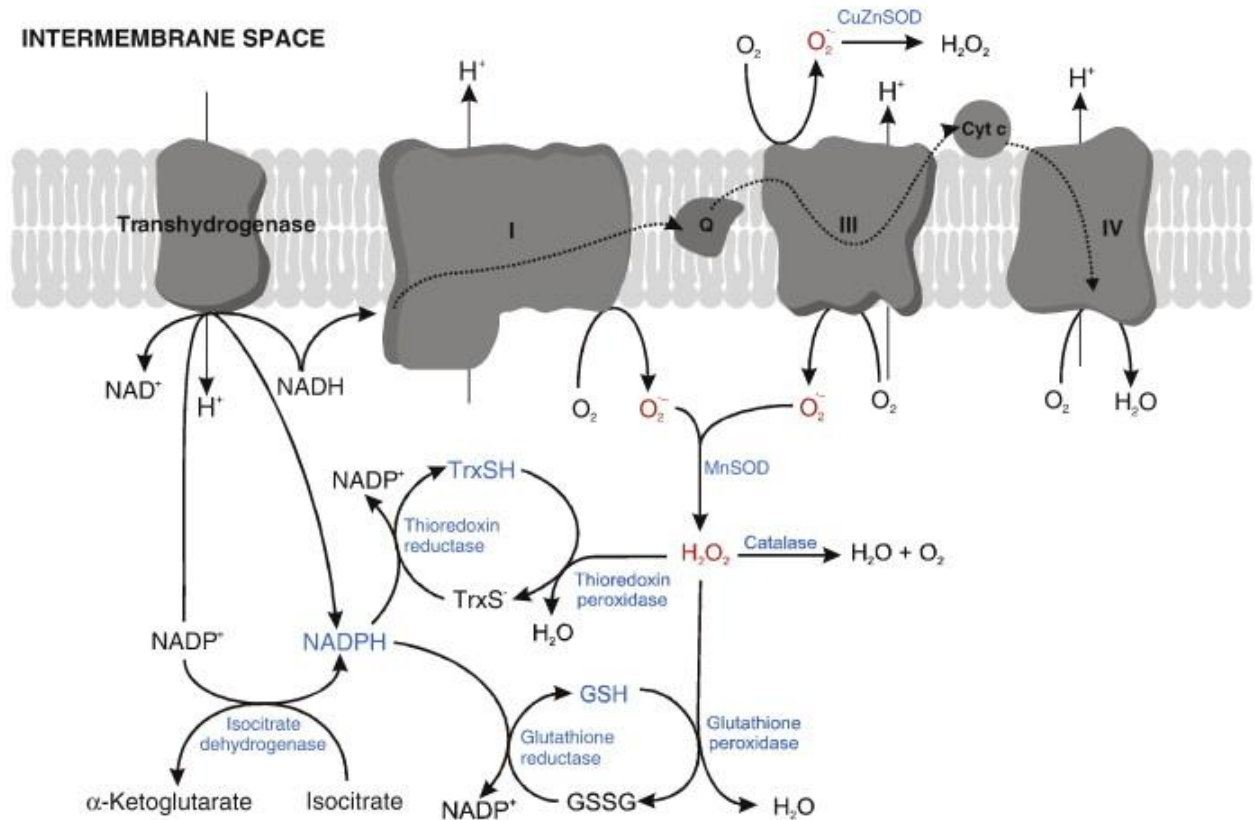


Figure 2.1 - Mitochondrial ROS (red) metabolism and endogenous antioxidant systems (blue). Superoxide radical anions ($O_2^{\cdot -}$) are formed by reduction of O_2 , mainly at Complexes I and III of the respiratory chain. $O_2^{\cdot -}$ is dismutated to H_2O_2 by CuZnSOD in the intermembrane space and Mn-SOD in the matrix. H_2O_2 can be removed by mitochondrial catalase or thiol peroxidases such as glutathione and thioredoxin peroxidase, using reduced glutathione (GSH) and thioredoxin (TrxSH) as substrate, respectively. Oxidized glutathione (GSSG) and thioredoxin ($TrxS^-$) are reduced by their respective reductases, using NADPH as an electron source. NADP can be kept reduced by the activity of the NAD/NADP transhydrogenase, with proton transport into the matrix, linking the inner membrane potential and the mitochondrial redox capacity. $NADP^+$ is also reduced by isocitrate dehydrogenase (Table from Kowaltowski et al., 2009).

2.2 Effects of Reactive Oxygen Species on Blood-Brain Barrier Function

It is apparent that BBB disruption is associated with many disease states which affect the CNS (see Chapter 1.5). Nearly all these diseases have an inflammatory and/or hypoxic component to them. This makes it essential to study how ROS produced during hypoxia or inflammation may lead to BBB disruption. A number of studies have linked ROS production to changes in BBB permeability, but few studies have looked at how ROS alter the TJ *in vivo*. The remainder of this section will briefly summarize studies on the impact of oxidative stress on BBB function.

A number of *in vivo* studies in several animal models of disease have indicated oxidative stress is involved in increased BBB permeability. In an animal model of stroke, BBB disruption was attenuated after one hour of reperfusion in NADPH oxidase knockout mice, indicating a role for $O_2^{\cdot -}$ generation in BBB damage during experimental stroke (Kahles et al., 2007). In a thromboembolic cortical ischemia model, mice overexpressing CuZnSOD exhibited reduced BBB permeability to Evans blue albumin (Kim et al., 2001). Evans blue leakage across the BBB was also reduced in hyperglycemic rats overexpressing human CuZnSOD following ischemia/reperfusion (Kamada et al., 2007). Albumin and horseradish peroxidase BBB permeability is reduced in cats pre-treated with SOD and catalase compared to untreated cats (Nelson et al., 1992). BBB permeability to serum albumin is increased following cardiac arrest in pigs and the permeability increase is reduced by the antioxidant methylene blue (Sharma et al.,

2010). Rats fed a diet deficient in the antioxidant vitamin E showed increased brain lipid peroxidation as well as greater BBB permeability to rhodamine B (Mohammed et al., 2008). It is also thought that BBB permeability, oxidative stress, and microglial activation play a key role in the pathogenesis of traumatic brain injury (Readnower et al., 2010). The lipid peroxidation inhibitor tirilazad mesylate protects against increased BBB permeability to Evans blue albumin following subarachnoid hemorrhage in rats (Smith et al., 1996). Oxidative stress is thought to play an important role in striatal BBB disruption in mice treated with the mitochondrial excitotoxin 3-nitropropionic acid. The BBB disruption seen in these mice is thought to be mediated by activation of MMP-9 by ROS (Kim et al., 2003). The psychoactive drug of abuse methamphetamine (METH) also increases BBB permeability to sodium fluorescein. This effect is reduced by administration of the antioxidant compound trolox (Ramirez et al., 2009).

In addition to the *in vivo* studies, a number of studies *in vitro* implicate ROS involvement in BBB disruption. Cultured cerebral endothelial cells exposed to hypoxia-reoxygenation mediated ROS production show a drop in TEER and a decrease in occludin expression. These effects are associated with activation of extracellular signal-regulated kinase (ERK1/2) (Krizbai et al., 2005). Ethanol decreases BBB integrity and increases ROS production and phosphorylation of occludin, claudin-5, and ZO-1 in brain microvessel endothelial cells (Haorah et al., 2005). These effects are reversed by antioxidants and thought to be mediated by degradation of basement membrane proteins by activated MMPs and protein tyrosine kinase-mediated phosphorylation of TJ

proteins (Haorah et al., 2007). Hydrogen peroxide increases paracellular permeability, increases occludin and actin expression, and causes redistribution of ZO-1 in bovine brain microvascular endothelial cells (Lee et al., 2004). Extracellular $O_2^{\cdot -}$ increases paracellular permeability through activation of the PI3 kinase and Protein kinase B (PKB) pathways via RhoA in brain endothelial cells (Schreibelt et al., 2007). These effects are associated with cytoskeletal rearrangements and the redistribution and disappearance of claudin-5 and occludin. 4-hydroxynoneal, a product of ROS-mediated lipid peroxidation, has been shown to increase BBB permeability to sodium fluorescein, sucrose, and dichlorokynurenic acid (Mertsch et al., 2001). Acetaminophen has also been shown to protect cultured brain endothelial cells against superoxide-induced oxidative stress (Tripathy and Grammas, 2009). In human brain endothelial cells, METH produces ROS, down-regulates occludin, and decreases TEER. These effects are attenuated by the antioxidant trolox (Ramirez et al., 2009).

2.3 Objectives and Hypothesis of the Present Study

The BBB is a dynamic system necessary for maintaining CNS homeostasis. The functional integrity of the BBB is compromised in numerous disease states. Studies in our laboratory have demonstrated that animal models of both hypoxia-reoxygenation (HR) and peripheral inflammatory pain (PIP) increase BBB paracellular permeability to ^{14}C -sucrose (Huber et al., 2001; Brooks et al., 2006; Witt et al., 2003). The TJ protein complexes which fuse together apposing brain microvascular endothelial cells are primarily responsible for restricting paracellular diffusion at the BBB. The

transmembrane protein occludin is a critical component of the TJ complex and our laboratory has shown that occludin exists as high molecular weight oligomeric assemblies in lipid raft regions of the plasma membrane at the TJ (McCaffrey et al., 2007). Occludin oligomeric assemblies are altered by HR and PIP. ROS are produced during HR and PIP and ROS production causes BBB disruption. The effects of ROS on the integrity of occludin oligomers at the BBB, however, has never been studied. **The major hypothesis of this study is that ROS produced during HR or PIP alter the functional integrity of the BBB by disrupting occludin oligomeric assemblies at the TJ.** In order to investigate this hypothesis, the following specific aims were addressed.

Specific Aim 1: Investigate the role of ROS on BBB functional integrity during HR and PIP.

Specific Aim 2: Investigate the role of ROS on the expression and localization of the TJ protein occludin during HR and PIP.

Specific Aim 3: Investigate the role of ROS on the integrity of occludin oligomeric assemblies in lipid rafts at the BBB TJ during HR and PIP.

CHAPTER 3

**ROLE OF REACTIVE OXYGEN SPECIES IN BLOOD-BRAIN BARRIER DISRUPTION DURING
HYPOXIA-REOXYGENATION**

3.1 Introduction

The blood-brain barrier (BBB) is a physical and metabolic barrier comprised of brain microvascular endothelial cells which restrict the passage of substances from the blood to the brain and help maintain brain homeostasis. The BBB expresses a high number of ion channels and transporters, has a low rate of pinocytosis, and forms intercellular tight junction (TJ) protein complexes which limit paracellular permeability (Hawkins and Davis, 2005). It has previously been shown that disruption of the BBB is associated with hypoxia and reoxygenation (HR) (Kaur and Ling, 2008). HR leads to an increase in BBB permeability (Witt et al, 2003), which may result in neurotoxic substances leaking from the blood into the brain and contributing to vasogenic edema. Cerebral HR is a central component of many disorders or conditions affecting cognition. These include stroke (Kalaria and Ballard, 2001), cardiac arrest (Lim et al, 2004), postoperative cognitive dysfunction (Caza et al., 2008), acute respiratory distress syndrome (Hopkins et al, 2006), obstructive sleep apnea (El-Ad and Lavie, 2005), high altitude cerebral edema and acute mountain sickness (Hackett, 1999).

Much of the cellular damage caused by hypoxic insult is thought to occur during the subsequent reoxygenation phase. HR is associated with an increased production of reactive oxygen species (ROS) (Wong and Crack, 2008). These ROS contribute to brain injury by reacting with proteins, lipids, and nucleic acids as well as by activating a number of redox sensitive signaling pathways. A number of different laboratories have shown that production of ROS can affect BBB permeability by a variety of mechanisms,

including modulation of TJ proteins (reviewed in Pun et al., 2009).

Previously, our laboratory showed that HR causes an increase in BBB paracellular permeability *in vivo* (Witt et al., 2003; Witt et al., 2008). This increase in BBB permeability correlates with alterations in the oligomeric assembly of the critical TJ protein occludin (McCaffrey et al., 2009). Occludin is a transmembrane protein which exists as oligomers in lipid raft regions at the plasma membrane of the BBB (McCaffrey et al., 2007). Multiple domains of occludin have previously been shown to regulate the diffusion of solutes across the TJ (Balda et al., 2000). Occludin oligomers are held together covalently by disulfide bonds (McCaffrey et al., 2009; Walter et al., 2009). These bonds can be disrupted by pathological conditions such as HR and inflammatory pain, leading to structural changes of the oligomers (McCaffrey et al., 2008; McCaffrey et al., 2009). Changes in the structure of occludin oligomers could potentially influence the ability of the TJ complexes to limit paracellular diffusion of molecules from the blood to the brain. This is the first study to look at the effects of oxidative stress on occludin oligomeric assembly at the BBB tight junctions, *in vivo*.

To examine the role that oxidative stress plays in disrupting the functional integrity of the BBB, we administered the stable, membrane permeable, water-soluble, nitroxide, tempol to rats before the induction of HR. Tempol shows superoxide dismutase-like activity towards the superoxide anion ($O_2^{\cdot-}$) as well as reactivity with the hydroxyl radical (OH^{\cdot}) (Saito et al., 2003), nitrogen dioxide (NO_2^{\cdot}), and the carbonate radical ($CO_3^{\cdot-}$) (Augusto et al., 2008). Tempol readily crosses the BBB (Zhelev et al., 2009)

and has previously been shown to provide neuroprotection as a free-radical scavenger in several models of brain injury and ischemia (Kwon et al, 2003; Deng-Bryant et al, 2008; Rak et al, 2000; Cuzzocrea et al, 2000).

In this dissertation, we looked at the effects of ROS produced during HR in a model that has previously been shown to induce alterations in BBB permeability and the structural integrity of the TJ protein occludin. We used the *in situ* brain perfusion method to assess functional BBB permeability following HR in animals pre-treated with tempol to examine the role of ROS in BBB disruption. In addition, we look at the effect ROS production has on occludin localization using confocal microscopy. Finally, we employ the method of density gradient fractionation of cerebral microvessels followed by SDS-PAGE electrophoresis under reducing and non-reducing conditions to examine the role ROS play in HR induced changes in the structural integrity of occludin.

3.2 Experimental Procedures

Radioisotopes, reagents, and chemicals

The [¹⁴C]-sucrose was purchased from American Radiolabeled Chemicals (St. Louis, MO).

Tempol was purchased from MP Biomedicals (Solon, OH). Ts-2 tissue solubilizer was purchased from Research Products International (Mt. Prospect, IL). Optiphase Supermix

scintillation cocktail was purchased from Perkin Elmer (Shelton, CT). EDTA-free

Complete Protease Inhibitors were purchased from Roche (Indianapolis, IN). OptiPrep

was purchased from Accurate Chemical (Westbury, NY). The Coomassie Plus Better

Bradford Assay Kit was purchased from Thermo Scientific (Rockford, IL). Rabbit anti-

occludin directed towards the C-terminus was purchased from Zymed (San Francisco, CA), Mouse anti-platelet-endothelial cell adhesion molecule 1 (PECAM-1) was purchased from AbD Serotec (Raleigh, NC). Mouse anti-heat shock protein 70 (HSP-70) was purchased from R&D Systems (Minneapolis, MN). Secondary antibodies for Western blotting and immunofluorescence were purchased from Amersham (Pittsburgh, PA) and Invitrogen (Carlsbad, CA) respectively. Western Lightning enhanced chemiluminescence reagent was purchased from Perkin Elmer (Shelton, CT). TO-PRO-3 and ProLong Gold were purchased from Invitrogen. XT sample buffer, XT reducing agent and Criterion gels were purchased from Bio-rad (Hercules, CA). All other antibodies or reagents, unless noted, were purchased from Sigma-Aldrich (St. Louis, MO).

Hypoxic Treatment

All experimental protocols were approved by the Institutional Animal Care and Use Committee at the University of Arizona. Adult female Sprague-Dawley rats (Harlan; Indianapolis, IN) weighing 230-280 g were housed under standard 12:12-h light-dark conditions and received food and water ad libitum. Rats were exposed to 6% O₂ for 1 hour, followed by 20 minutes of reoxygenation. 10 minutes prior to hypoxic treatment, rats were given an intraperitoneal (i.p.) injection of saline or tempol (200 mg/kg body weight).

In Situ brain Perfusion

The *in situ* brain perfusion technique was adapted from previously published methods

(Zlokovic et al, 1986; Takasato et al, 1984) and was performed as previously described (Witt et al, 2003). After the hypoxic insult (6% O₂, 1 h), rats were anesthetized with a 1.0 ml/kg i.p. injection of an anesthetic cocktail consisting of ketamine (78.3 mg/ml), xylazine (3.1 mg/ml), and acepromazine (0.6 mg/ml) and allowed to reoxygenate for 20 min in room air (21% O₂) prior to infusion with the paracellular permeability marker ¹⁴C-sucrose (MW=342). Surgery was performed during the reoxygenation phase. Once anesthetized, the rats were heparinized (10,000 U/kg) and the carotid arteries were isolated and cannulated with silicon tubing. The perfusion medium contained albumin-bound Evans blue dye in a mammalian Ringer solution [117.0 mM NaCl, 4.7 mM KCl, 0.8 mM MgSO₄·H₂O), 24.88 mM NaHCO₃, 1.2 mM KH₂PO₄, 2.5 mM CaCl₂·6H₂O, 10 mM D-glucose, 39 g/l dextran (MW 70,000) and 1 g/l BSA] which was bubbled with 95%O₂/5%CO₂ gas mix. The Ringer solution was filtered, heated (37°C), and de-bubbled before arterial infusion at 3.1 ml/min. The paracellular permeability marker ¹⁴C-sucrose was infused into the perfusate inflow at 0.5 ml/min for 10 min, followed by a 1 min washout containing Ringer with no radioactive tracer to clear the vascular space of radioactivity.

At the end of the perfusion, the rat was decapitated and the brain was removed. The meninges and choroid plexuses were removed and the brain was divided and placed into pre-weighed vials. 1 ml of tissue solubilizer was added to each vial and allowed to dissolve the brain sample for 48 h. After solubilization, 100 ul of 30% glacial acetic acid was added to each sample to quench chemiluminescence. 2.5 ml of Optiphase Supermix

scintillation cocktail was added to each sample. Triplicate samples of 100 μ l aliquots of the perfusion medium was treated in the same manner as the perfused brain samples. All samples were then measured for disintegrations per minute (dpm) (1450 LSC and Luminescence Counter, Perkin Elmer; Waltham MA). The ratio of the concentration of ^{14}C -sucrose in tissue (C_{brain} , in dpm/g) was compared to perfusate ($C_{\text{perfusate}}$, in dpm/ml) and expressed as a percent ratio $R_{\text{brain}} = (C_{\text{brain}}/C_{\text{perfusate}}) \times 100\%$. We have previously used capillary depletion analysis in this model to show that the increase in ^{14}C -sucrose following HR was not due to increased trapping within the microvascular endothelial cells (Witt et al, 2003).

Microvessel enrichment and fractionation

After hypoxic or control treatment, rats were anesthetized with a 1.0 ml/kg i.p. injection of an anesthetic cocktail consisting of ketamine (78.3 mg/ml), xylazine (3.1 mg/ml), and acepromazine (0.6 mg/ml). They were then decapitated after 20 min reoxygenation and the brains were extracted. The cerebellum, meninges and choroid plexuses were removed and the cerebral hemispheres were homogenized in 4 ml of microvessel isolation buffer A [103 mM NaCl, 4.7 mM KCl, 2.5 mM CaCl_2 , 1.2 mM KH_2PO_4 , 1.2 mM MgSO_4 , 15 mM HEPES, 2.5 mM NaHCO_3 , 10 mM D -glucose, 1 mM sodium pyruvate, pH 7.4]. 4 ml of ice-cold buffer A with 26% dextran was added to the homogenates which were vortexed and centrifuged at 5800g for 10 min at 4° C and repeated. Pellets were resuspended in buffer A supplemented with protease inhibitors (Roche EDTA-free Complete Protease Inhibitor, 2 mmol/L PMSF, 1 mmol/L Na_3VO_4 , 1 mmol/L NaF and 1

mmol/L sodium pyrophosphate) then passed through a 100 μ m filter. The filtrate was then passed through a 40 μ m filter. The microvessels remaining on the filter were collected in buffer A and centrifuged at 1500 g for 10 min. A small aliquot of these microvessels was placed on a glass slide and immunostained as below. The pellet from the remaining microvessels was then resuspended in 4 ml of buffer B [20 mM tris-HCl, 250 mM sucrose, 1 mM CaCl₂, 1 mM MgCl₂, pH 7.4] with protease inhibitors and drawn through a 21 G needle 20X. The protein concentration of each sample was then determined using the Coomassie Plus Better Bradford Assay Kit and equal amounts of microvessel homogenates were mixed with 50% OptiPrep in buffer B. This suspension was layered beneath a discontinuous 0/5/10/15/20% Optiprep gradient (prepared in buffer B without ions) then centrifuged for 90 min at 52,000 g at 4°C. 1 ml fractions were collected from the top of the gradient using a Biocomp Gradient Station *ip* (Fredericton, Canada). Each fraction was then assayed for refractive index (density) and protein content using the Coomassie Plus Better Bradford Assay Kit.

Western Blot Analysis

Equal volume aliquots of each gradient fraction were mixed with equal volumes of 2X perfluoro-octanoic acid (PFO) extraction buffer (100 mM Tris, 20% glycerol, 4% PFO, pH 8.0) and allowed to incubate at 25° C for 30 min. Samples were then centrifuged at 11,000 g for 10 min and supernatants containing PFO-solubilized material were added to 4X XT sample buffer with or without XT reducing agent containing tris(2-carboxy-ethyl)phosphine hydrochloride (TCEP). Each fraction was then incubated at 70° C for 10

min before undergoing SDS-PAGE on 10% Bis-Tris Criterion gels. Sets of gels (reducing and non-reducing, for each treatment condition) were then transferred to the same PVDF membranes, blocked in 5% milk, and incubated overnight in 1° antibody (1:1000 dilution). Blots were then washed, incubated in HRP-conjugated 2° antibody and detected using enhanced chemiluminescence reagent. Each blot was stained with Coomassie and the optical density (OD) of each band was normalized to the total protein in the lane according to previously published methods (Aldridge et al, 2008). Densitometry was performed using ImageJ software (Wayne Rasband, Research Services Branch, National Institutes of Mental Health, Bethesda, MD).

Immunofluorescence

All slides from control and treated animals were collected and processed in parallel. Primary antibody was omitted on some slides as a negative control. Fluorescent immunostaining for occludin was performed on microvessel preparations enriched as above. Briefly, microvessels were heat-fixed on glass slides at 95° C for 10 min, followed by fixation in ice-cold acetone for 10 min. The slides were blocked in 2% goat serum and 1% BSA before incubation in rabbit anti-occludin primary antibody (1:250) and the endothelial specific marker mouse anti-PECAM-1 (1:1000) overnight in the cold, slides were incubated with the appropriate Alexafluor-conjugated secondary antibodies.

For HSP-70 immunostaining, microvessels were placed on a glass slide and allowed to air dry before being fixed in 3.7% formaldehyde for 10 min. The microvessels

were permeabilized in 0.1% Triton x-100, blocked as above and incubated overnight in the cold in mouse anti-HSP 70 (1:400) and the endothelial specific marker rabbit anti-von Willebrand Factor (1:5000). The slides were then incubated with the appropriate Alexafluor-conjugated secondary antibodies.

For Hif-1 α immunostaining, microvessels were placed on a glass slide and allowed to air dry before being fixed in ice-cold acetone for 10 min. The slides were blocked as above and incubated in mouse anti-Hif-1 α (1:200) along with rabbit anti-von Willebrand Factor (1:5000) overnight in the cold. Slides were then incubated with the appropriate Alexafluor-conjugated secondary antibodies. The nucleus of the microvessels was then stained with the nuclear-specific dye TO-PRO-3 (10 μ M) for 10 min. All slides were mounted in ProLong Gold anti-fade reagent before applying the coverslip.

Confocal Microscopy

All slides were imaged on a Zeiss LSM 510 meta-NLO confocal microscope with filters appropriately set to avoid bleed-through. Only microvessels positive for the endothelial-specific markers PECAM-1 or von-Willebrand Factor were used for analysis. Semi-quantitative analysis of the mean fluorescent intensity of HSP-70 was performed according to previously published methods (Hawkins et al, 2004). Microvessels were randomly chosen from animals in each treatment group and the mean fluorescence intensity was analyzed using Zeiss LSM Image Browser software with the data expressed

as a percentage of control. To investigate Hif-1 α translocation to the nucleus, the Mander's Colocalization coefficient for Hif-1 α and TO-PRO-3 was determined using the Zeiss LSM Image Browser software in randomly chosen microvessels in each treatment group.

Statistical Analysis

All data analysis was performed using SigmaPlot software. To determine statistical significance between treatment groups, data was analyzed using one-way ANOVA, followed by Bonferroni's t-test. Data are presented as means \pm SE. A value of $P < 0.05$ was accepted as statistically significant.

3.3 Results

Hif-1 α Expression and Translocation to the Nucleus

Hif-1 α is an oxygen-sensitive protein which is continuously synthesized and degraded under normoxic conditions. Under hypoxic conditions, degradation of Hif-1 α decreases and translocation to the nucleus occurs where Hif-1 α heterodimerizes with Hif-1 β and binds to hypoxia responsive elements (HREs) of target genes. Our confocal imaging data (Figure 3.1) on our enriched microvessel preparations shows that HR causes an increase in Hif-1 α colocalization with the nuclear dye TO-PRO-3, suggesting Hif-1 α translocation to the nucleus due to hypoxia. We measured the ratio of nuclear Hif-1 α to total Hif-1 α using the Mander's colocalization coefficient (Table 3.1). A value of 0 indicates no colocalization of Hif-1 with the nucleus while a value of 1 indicates that all pixels

colocalize. We obtained a Mander's colocalization coefficient of 0.142 ± 0.0019 for Nx+S and 0.119 ± 0.015 for Nx+T. HR+S treated rats showed a statistically significant increase in Hif-1 α nuclear colocalization with a Mander's colocalization coefficient of 0.211 ± 0.22 over normoxic animals. HR+T treated rats had a Mander's colocalization coefficient of 0.154 ± 0.012 . Images are representative of six rats per treatment group (n=6).

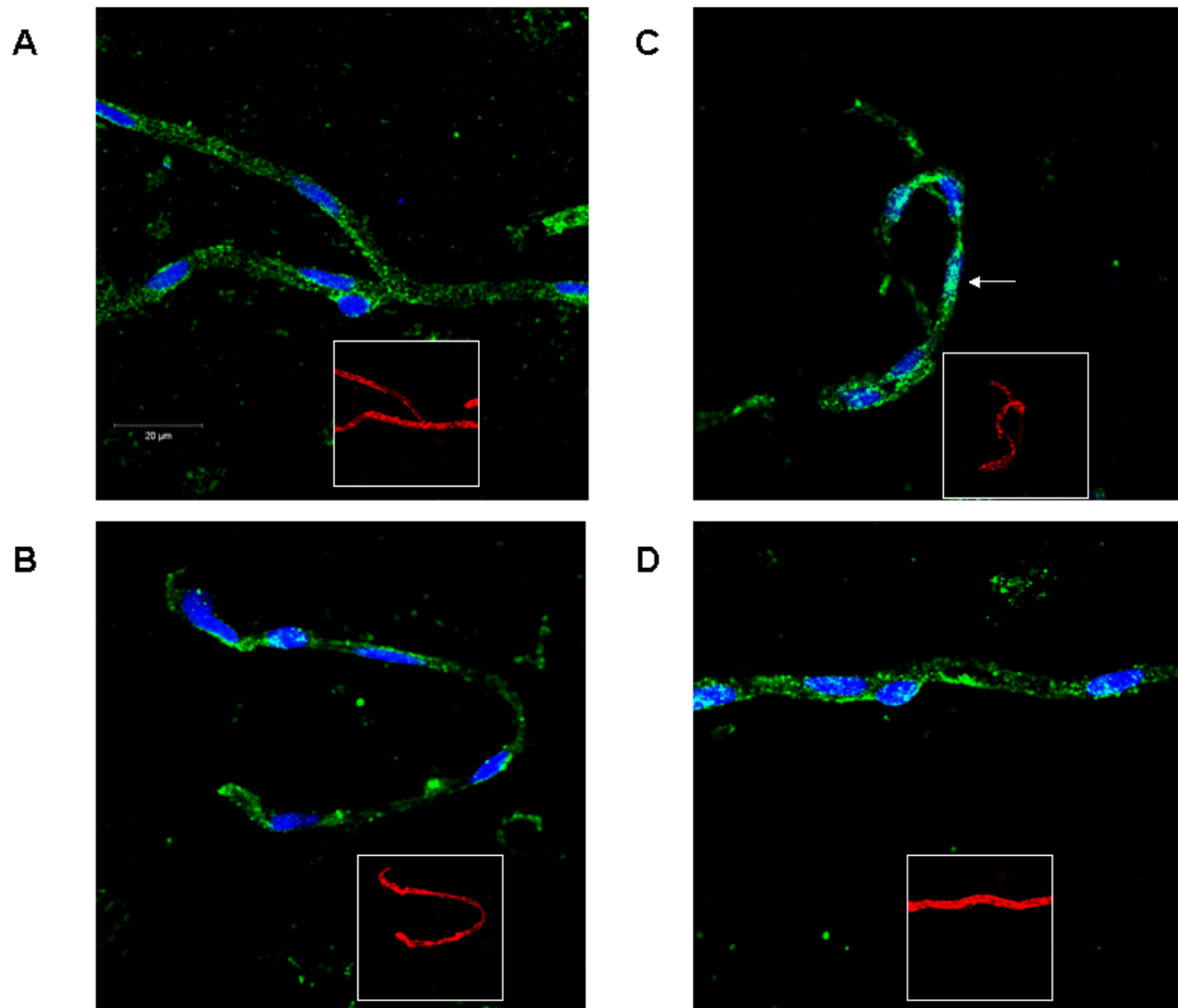


Figure 3.1 Hypoxia and reoxygenation (HR) induces hypoxia-inducible factor 1 α (Hif-1 α) translocation to the nucleus. Immunofluorescence of Hif-1 α (green) and the nuclear dye TO-PRO-3 (blue) in brain microvessels of normoxic (Nx) plus saline (A), Nx plus tempol (B), HR plus saline (C), and HR plus tempol (D)-treated rats. Rats exposed to HR show an increase in translocation of Hif-1 α to the nucleus (arrow). Immunofluorescence of the endothelial-specific marker von Willebrand factor (red) is shown in the inset.

Table 3.1 Mander's colocalization coefficients for Hif-1 α and TO-PRO-3

Nx+S	Nx+T	HR+S	HR+T
0.142 \pm 0.019	0.119 \pm 0.015	0.211 \pm 0.022 ^{*,#}	.154 \pm 0.012

Cerebral microvessels from animals exposed to normoxia (Nx) or hypoxia-reoxygenation (HR) with saline (S) or tempol (T) were analyzed for colocalization of Hif-1 α with the nuclear dye TO-PRO-3. HR+S treated rats show a significant increase in Hif-1 α nuclear colocalization compared to normoxic rats. Data are representative of 50-60 randomly chosen microvessels from each treatment group. Values are means \pm SE. One-way repeated measures ANOVA and the *post hoc* Bonferonni t-test was used to establish significance. * $p < 0.05$ vs. Nx+S, # $p < 0.01$ vs. Nx+T

HSP-70 Expression

Up-regulation of HSP-70 is associated with oxidative stress (Ronaldson and Bendayan, 2008; Amadio et al, 2008). We looked at levels of HSP-70 in the enriched microvessel preparations of all treatment groups using confocal microscopy (Figure 3.2A). Images are representative of six rats per treatment group (n = 6). Our data shows a significant increase in HSP-70 (1.5-fold) mean fluorescence intensity resulting from HR. Tempol (HR+T) attenuated this increase (1.2-fold), indicating reduced levels of cellular stress due to scavenging of free radicals during HR (Figure 3.2B).

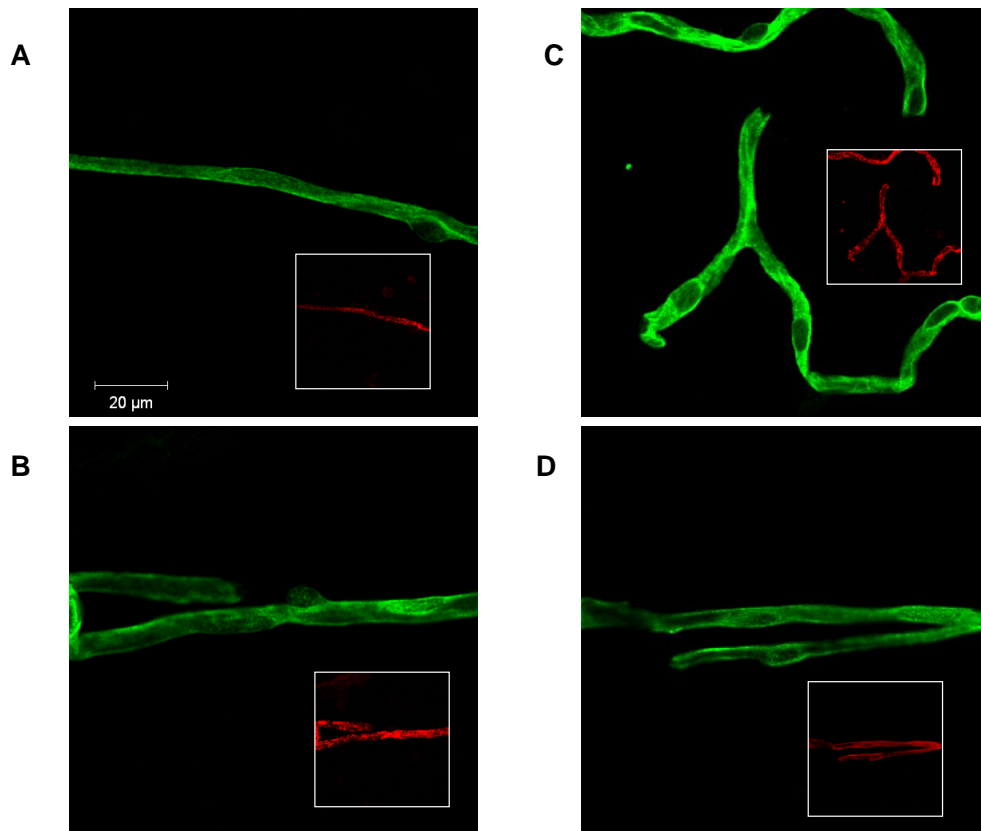
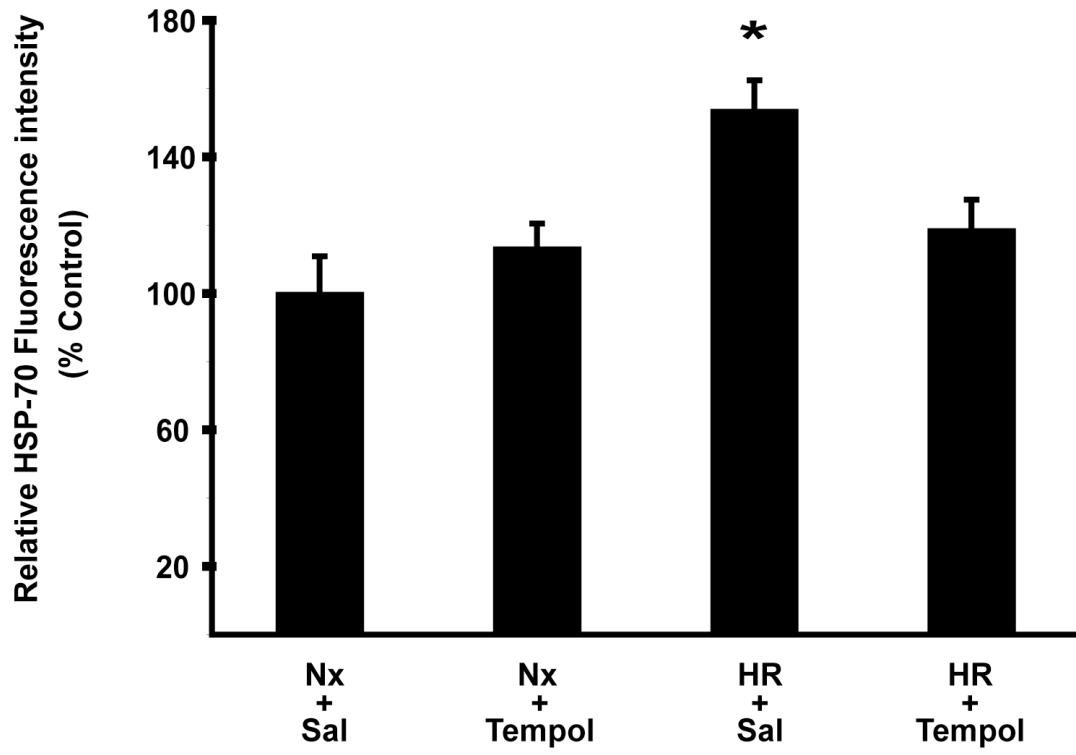


Figure 3.2 Oxidative stress induces expression of heat shock protein (HSP-70). Immunofluorescence of HSP-70 (green) in brain microvessels of normoxic (Nx) plus saline (Nx+S) (A), Nx plus tempol (Nx+T) (B), hypoxia–reoxygenation (HR) plus S (HR+S) (C), and HR + T (D)-treated rats. Rats exposed to HR show an increase in HSP-70 immunofluorescence. Tempol attenuated this increase. Immunofluorescence of the endothelial-specific marker von Willebrand factor (red) is shown in the inset. (E) Mean fluorescence intensity of HSP-70 in all treatment groups expressed as a percent control. * $P < 0.05$ versus HR+T and Nx+T. $P < 0.01$ versus Nx+S ($n = 28$ to 33 microvessels per treatment group).

E



In Situ Brain Perfusion

The role of oxidative stress in altering BBB permeability during HR was investigated using the *in situ* brain perfusion technique. This method maintains a constant cerebral flow rate of perfusion fluid and eliminates potential confounding variables associated with peripheral blood flow, metabolism, and clearance. ^{14}C -sucrose was used as a marker of paracellular permeability due to its minimal BBB penetration under physiological conditions and its inherent metabolic stability in this system. The ^{14}C -sucrose was not subject to any metabolism during the perfusion as verified by HPLC analysis (data not shown). In Normoxia + saline treated (Nx+S) rats, the Rbr was $1.60\% \pm 0.09\%$ (Figure 3.3). After HR, the Rbr was $2.43\% \pm 0.25\%$ which was significantly increased ($P=0.016$) by 51.9% compared to control. With administration of the free radical scavenger tempol 10 min before HR, the Rbr was $1.61\% \pm 0.15\%$, which was significantly lower than the Rbr from the HR + saline treated animal ($P=0.014$). This suggests that ROS are involved in the increase in BBB permeability associated with H/R. The Nx animals administered tempol (Nx+T) showed a nonsignificant increase in Rbr of $1.92\% \pm 0.15\%$ compared to normoxic animals administered saline (Figure 3.3).

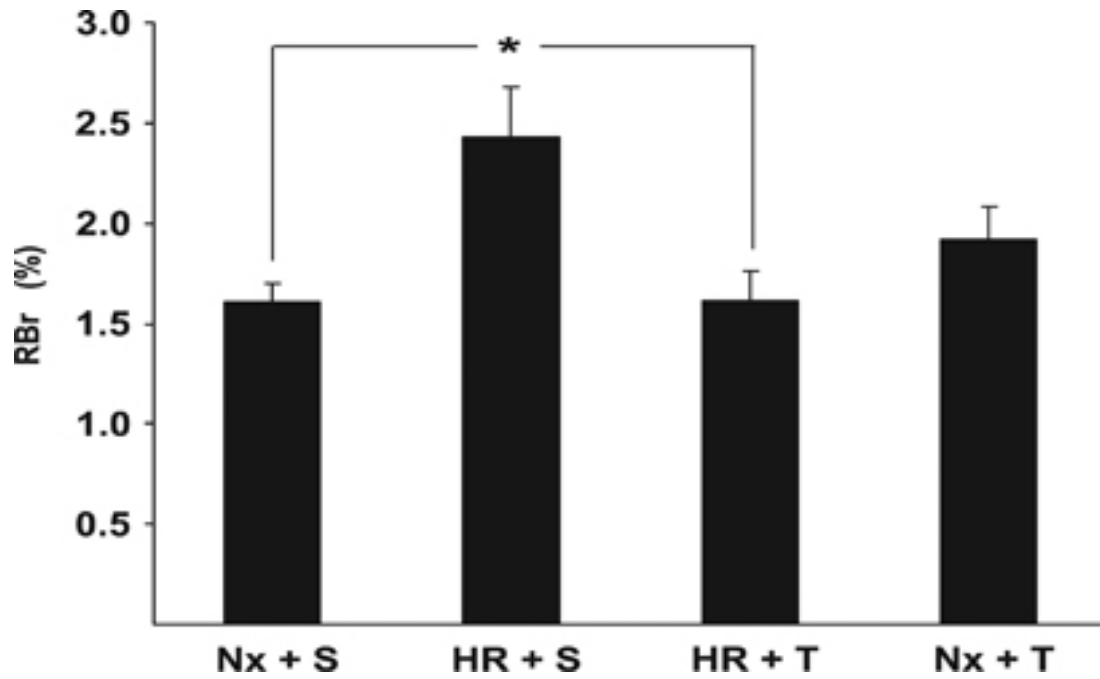


Figure 3.3 Effects of hypoxia and reoxygenation (HR) and tempol treatment on BBB permeability to ^{14}C -sucrose. After treatment, normoxia (Nx) plus saline (S) (Nx+S), Nx plus tempol (T) (Nx+T), HR+S, and HR+T rats were anesthetized and subjected to *in situ* brain perfusion for 10 mins with ^{14}C -sucrose. The amount of radioactivity in the brain versus the perfusate was expressed as Rbr%. Results are expressed as mean \pm s.e. * $P<0.05$.

Occludin Microvascular Distribution

To examine the effects of H/R and oxidative stress on the cellular localization of the TJ protein occludin, enriched microvessels preparations were placed on glass slides and stained for occludin. Slides were then examined under a laser scanning confocal microscope. Images are representative of five animals per treatment group (n = 5). In microvessels isolated from Nx animals, there was continuous staining of occludin along the margins of intercellular contact (Fig. 3.4A). After HR treatment, an increase in intracellular punctate staining of occludin was observed, indicating a change in localization of occludin away from the TJ complex. Animals treated with tempol prior to H/R showed continuous staining of occludin along the TJ similar to what was seen in the normoxic animals. The number of microvessels exhibiting punctate staining in each treatment group was quantitated and is presented in Table 3.2. Microvessels in Nx+S rats showed punctate staining in $14.95\% \pm 2.11\%$ of microvessels. HR+T and Nx+T rats exhibited punctate staining in $15.94\% \pm 0.42\%$ and $16.60\% \pm 2.09\%$ respectively. In HR+S treated rats, $28.74\% \pm 3.21\%$ of microvessels showed punctate staining, a statistically significant increase compared to the other treatment groups ($P < 0.01$). These results indicate that oxidative stress induces a change in occludin intracellular localization.

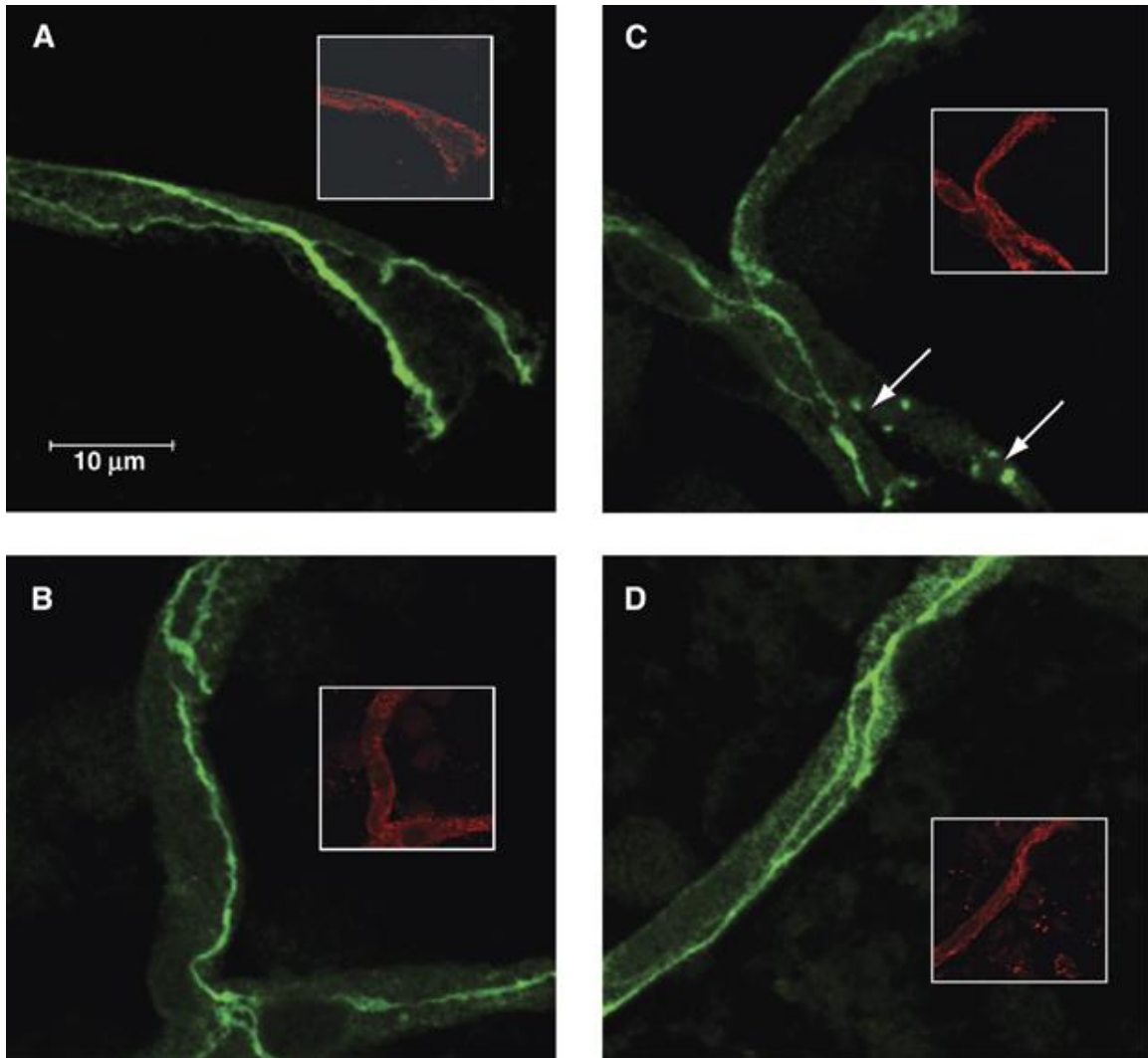


Figure 3.4 Oxidative stress induces changes in occludin localization. Immunofluorescence of occludin (green) and the endothelial-specific marker platelet-endothelial cell adhesion molecule 1 (PECAM-1) (red inset) in brain microvessels of normoxic (Nx) plus saline (**A**), Nx plus tempol (**B**), hypoxia–reoxygenation (HR) plus saline (**C**), and HR plus tempol (**D**). HR induces an increase in punctate staining of occludin (arrows), suggesting the movement of occludin away from the tight junction. Tempol prevents this increase, indicating that oxidative stress is involved in altering the cellular localization of occludin.

Table 3.2 Percentage of Cerebral Microvessels Exhibiting Punctate Staining of Occludin

N+S	N+T	HR+S	HR+T
14.95% ± 2.11%	16.60% ± 2.09%	28.74% ± 3.21%*	15.94% ± 0.42%

Microvessels were analyzed for punctate staining in normoxia + saline (Nx+S), normoxia + tempol (Nx+T), hypoxia-reoxygenation + saline (HR+S) and hypoxia-reoxygenation + tempol (HR+T). Values are means ± SE; n = 500 microvessels per treatment group. One-way repeated measures ANOVA and the *post hoc* Bonferonni t-test was used to establish significance. * $p < 0.01$ compared to N+S, N+T, and HR+T.

Density Gradient Fractionation

Density gradient centrifugation and fractionation of intact microvessels was performed to examine the distribution of occludin within plasma membrane microdomains. The protein concentration and refractive indices from intact microvessels subjected to density gradient fraction are presented as averages of 3 separate experiments, each containing 3 rats per treatment group (Figure 3.5A). Our data shows that the protein concentration and refractive index from each fraction is similar for each treatment group. This demonstrates our analysis was performed on membrane microdomains which are similar across all treatment groups. We have previously shown that the TJs exist primarily in fractions 7 & 8 (McCaffrey et al, 2007). Using SDS-PAGE, we analyzed Western blots of fractions 7 & 8 under reducing and non-reducing conditions to investigate the band patterns of PFO-soluble occludin oligomers (Figure 3.5B). PFO has previously been shown to preserve the oligomeric structure of membrane proteins by stabilizing internal non-covalent interactions between component protein subunits (Ramjeesingh et al, 1999). During HR, a significant increase in the optical density of occludin oligomers under non-reducing conditions compared to normoxic controls (4.9-fold in fraction 7 and 11.0-fold in fraction 8) is observed (Figure 3.5C). Occludin oligomers exhibit a broad, intense staining pattern resulting from HR. This suggests

extensive conformational changes in occludin occur during HR. Administration of tempol before HR served to significantly decrease the extent of oligomeric disassembly and to attenuate the increase in optical density of non-reduced occludin oligomeric isoforms compared to Nx+S rats (2.1-fold in fraction 7 and 4.1-fold in fraction 8). Comparison of occludin banding patterns on non-reducing with reducing blots reveals that the reducing agent TCEP increases the detection of occludin oligomeric isoforms in Nx animals, but not in HR animals. This suggests that HR causes conformational changes of occludin oligomeric assemblies, exposing more of the structure to antibody.

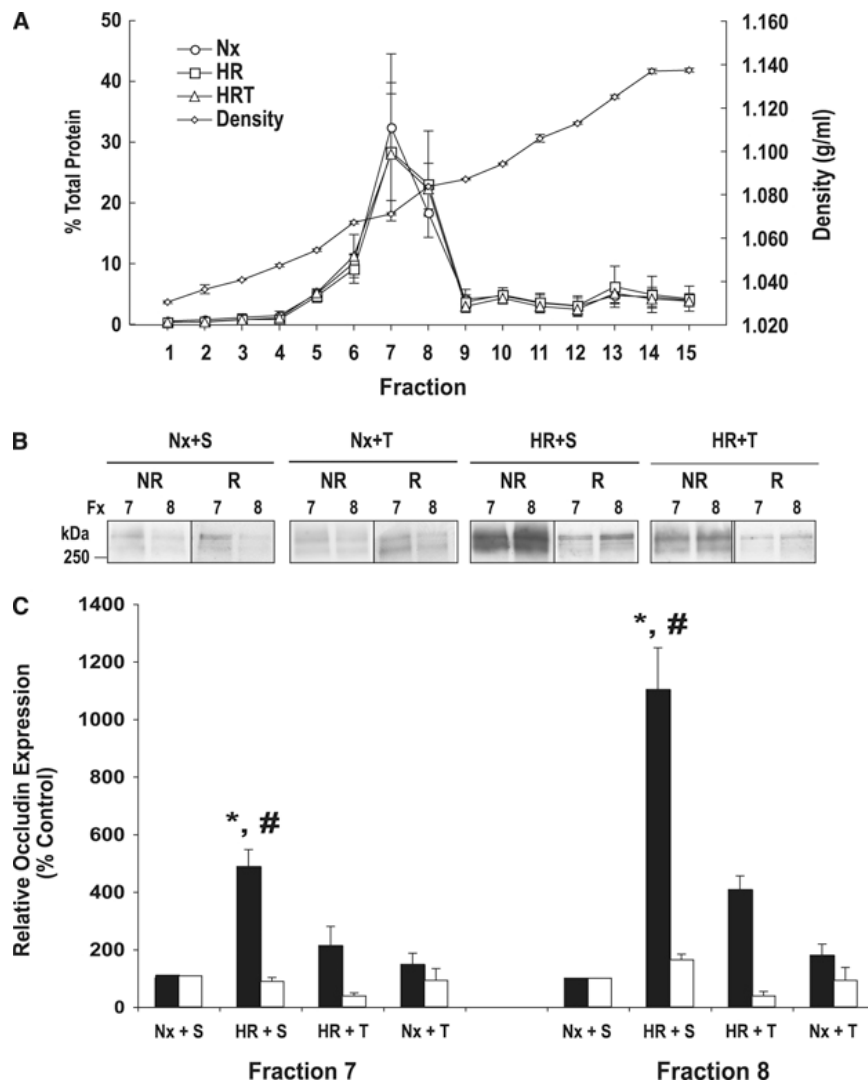


Figure 3.5 Density gradient fractionation of cerebral microvessels. **(A)** Profiles of protein concentrations and refractive indices (density) of cerebral microvessels after fractionation in normoxia (Nx) plus saline (S) (Nx+S), Nx plus tempol (T) (Nx+T), hypoxia-reoxygenation (HR) + S (HR+S), and HR+T. **(B)** Representative sodium dodecyl sulfate polyacrylamide gel electrophoresis (SDS-PAGE) and western blot of occludin oligomers in fractions 7 and 8 under nonreducing (NR) and reducing (R) conditions. Fractions 7 and 8 have previously been shown to be associated with the tight junction in lipid rafts at the plasma membrane. **(C)** Western blot analysis of occludin oligomers in fractions 7 and 8 under reducing and nonreducing conditions. Data are presented as mean \pm s.e. and are representative of three separate experiments with three rats pooled in each treatment group. * $P < 0.001$ versus Nx+S and Nx+T; $P < 0.01$ versus HR+T in fraction 7. * $P < 0.01$ versus Nx+S and Nx+T; $P < 0.05$ versus HR+T in fraction 8.

3.4 Discussion

The BBB plays a critical role in maintaining CNS homeostasis. Inability of the BBB to perform its normal physiological functions is thought to contribute to numerous disease states affecting the CNS, many of which have an HR component (Hawkins and Davis, 2005; Zlokovic 2008). Cerebral HR occurs during stroke and microvascular infarcts, vascular dementia, cardiac arrest, postoperative cognitive dysfunction, acute respiratory distress syndrome, obstructive sleep apnea, and high altitude cerebral edema. We have previously shown that HR causes an increase in paracellular permeability at the BBB (Witt et al., 2003; Witt et al., 2008). We have also shown changes in occludin protein localization and oligomeric assemblies that are associated with HR (McCaffrey et al., 2009). Oligomers of occludin are key components of the TJ protein complexes which are critical for restricting paracellular diffusion of solutes from the blood to the brain. Little is known about the mechanisms that lead to changes in occludin oligomeric assembly at the BBB following HR. HR is associated with a production of ROS which can lead to oxidative stress and BBB disruption (Pun et. al., 2009). Recent evidence indicates that the oligomerization of occludin is redox sensitive (Walter et al, 2009). These observations led us to investigate the influence of oxidative stress on BBB permeability and occludin structural integrity during HR. In order to examine this possibility, we used the free radical scavenger tempol to pharmacologically inhibit production of ROS.

In order to confirm that the brains of rats exposed to our HR treatment are

indeed hypoxic, we stained isolated microvessels for Hif-1 α . Hif-1 α is a transcription factor that is constitutively degraded under normoxic conditions. Hypoxia causes Hif-1 α to stabilize, which allows it to translocate to the nucleus, dimerize with Hif-1 β , and regulate gene transcription. Our confocal microscopy data shows increased colocalization of Hif-1 α with the nuclear dye TO-PRO-3 in HR treated animals, which indicates that Hif-1 α is stabilized and does translocate to the nucleus in response to HR. HR does not cause a significant increase in animals pre-treated with tempol. This may be due to an increase in ROS production during HR. ROS have previously been shown to induce Hif-1 α nuclear translocation independent of hypoxia (Haddad and Land, 2001). Since tempol acts as a ROS scavenger, our data suggests that the translocation of Hif-1 α to the nucleus was attenuated due to a decrease in ROS production in HR+T rats.

As a marker of cellular stress, we also stained microvessels for HSP-70. HSP-70 has previously been shown to be up-regulated due to stressors such as hypoxia and/or oxidative stress. Our data shows prominent HSP-70 immunoreactivity in the brain microvasculature during HR; however, pre-treatment with tempol attenuated the HR-associated increase in HSP-70 expression. This suggests a reduction in cellular stress in the brains of rats administered tempol.

Using the *in situ* brain perfusion technique, we examined the role of oxidative stress on BBB permeability following an acute exposure to HR *in vivo*. This technique has advantages over other techniques of perfusion or injection of solutes such as the brain uptake index (BUI) technique (Zlokovic et al, 1985). The *in situ* brain perfusion technique

is much more sensitive than techniques employing single pass extraction. It also avoids confounding physiological variables such as differences in blood pressure and peripheral metabolism and allows one to measure permeability of substances directly at the BBB (Martel et al, 1997). Using ^{14}C -sucrose as a marker of paracellular permeability (Bhattacharjee et al, 2001), we found that administration of tempol 10 min before HR treatment prevented the increase in BBB permeability associated with HR. This suggests that oxidative stress mediates the increase in BBB permeability seen in our model of acute HR. There was also a slight but nonsignificant increase in BBB permeability in Nx animals administered tempol (Nx+T). Tempol has been shown to increase bioavailability of nitric oxide (NO) which reacts with O_2^- under physiological conditions to produce peroxynitrite (ONOO-) (Zollner et al, 1997) . Elevated levels of NO have previously been shown to increase BBB permeability *in vitro* and *in vivo* (Mark et al, 2004; Boje and Lakhman 2000). Therefore, the high dose of tempol used in this study may have scavenged O_2^- and reduced the number of free radicals available to interact with NO. This pharmacological effect of tempol may lead to an increase in BBB permeability mediated by NO under physiological conditions.

Paracellular permeability at the BBB is regulated mainly by the TJs. Our data showing tempol prevents the increase in BBB permeability to ^{14}C -sucrose after HR treatment suggests that oxidative stress may also affect the molecular structure of the TJs. Previous work by our laboratory has indicated that the TJ protein occludin is affected by HR (McCaffrey et al, 2009) and its ability to oligomerize is redox sensitive

(Walter et al, 2009). These observations led us to investigate the effects of oxidative stress on occludin at both the cellular and molecular level using confocal microscopy and density gradient subcellular fractionation followed by Western blot analysis.

Confocal microscopy of isolated cerebral microvessels immunostained for occludin revealed continuous distribution of occludin along the margins of the TJ. HR induced intracellular punctate staining of occludin in regions of the microvessel not associated with TJs. In contrast, microvessels from HR+T rats show staining of occludin at the TJ in a pattern similar to Nx+S rats, suggesting that tempol may prevent HR associated changes in occludin localization. Taken together, our data imply that oxidative stress may induce changes in the cellular localization of occludin at the BBB.

We have previously used a detergent-free density gradient centrifugation method to examine the distribution of occludin in plasma membrane microdomains of cerebral microvessels. These studies have revealed valuable insight into the structure of occludin at the BBB. Density gradient fractionation of intact microvessels has shown that occludin exists in the TJ associated lipid raft regions corresponding to fractions 7 & 8 where it colocalizes with the lipid raft marker caveolin-1 and the TJ marker Rab-13 (McCaffrey et al, 2007). We have also used PFO (which stabilizes the quaternary structure of protein complexes) to solubilize occludin oligomeric assemblies (Ramjeesingh et al, 1999). Extracts of PFO soluble occludin subjected to non-reducing PFO-PAGE have revealed that in TJ associated fractions 7 & 8, occludin exists almost exclusively as high molecular weight (HMW, >250 kDa) oligomers (McCaffrey et al,

2009). It is only when occludin is solubilized in SDS and/or subjected to reducing conditions that lower molecular weight isoforms are detected. These data strongly suggest that occludin exists as HMW oligomeric assemblies at the TJs of the BBB *in vivo*. We have also shown through the use of hydrophobic and hydrophilic reducing agents that these occludin oligomeric assemblies are held together by disulfide bonds (McCaffrey et al, 2007). It has been shown that the C-terminus of the occludin molecule is involved in forming these disulfide bonds and the formation of these bonds is redox sensitive (Walter et al, 2009). These observations led us to investigate the effects of oxidative stress on the structural integrity of HMW occludin oligomers.

Using a C-terminal antibody to occludin, we subjected equal amounts of protein in fractions 7 & 8 to SDS-PAGE under non-reducing and reducing conditions. Our data show very faint banding patterns of occludin oligomeric assemblies located primarily in fraction 7 of Nx animals. Under reducing conditions with the hydrophilic reducing agent TCEP, these bands become much more intense. This suggests that under non-reducing conditions, the antigen is less accessible to antibody, presumably because it is being masked. Reducing conditions cleave these disulfide bonds and allow the antibody greater access to the antigen. Remarkably, oligomeric assemblies of occludin can still be detected after occludin has been subjected to SDS-PAGE under hydrophilic reducing conditions. This suggests an inner core of hydrophobic disulfide bonds holding the oligomeric assemblies together. In contrast to what was observed in Nx rats, HR rats show a prominent band of occludin oligomers under non-reducing conditions. This data

suggests the antibody binds to non-reduced occludin more readily in rats subjected to HR. This indicates that HR may induce conformational changes in occludin oligomers, possibly through the cleavage of disulfide bonds. In addition, occludin redistributes from fraction 7 to the higher density fraction 8 in the HR rats. Taken together, these data suggest that HR affects both the localization and the structural integrity of occludin oligomeric assemblies. Tempol-treated HR rats show significantly less dense bands of occludin oligomers under non-reducing conditions compared with HR+S rats. This suggests that oxidative stress is involved in the conformational changes of occludin oligomeric assemblies and free radical scavengers such as tempol can preserve the structural integrity of occludin at the BBB during an HR insult.

In summary, our data suggests that oxidative stress during HR may cause disruption of the BBB, leading to an increase in permeability to ¹⁴C-sucrose. In addition, ROS may cause changes in localization and structure of the TJ protein occludin. Both the structure and the localization of occludin are critically important to its function in maintenance of the BBB's ability to restrict permeability to solutes in the systemic circulation. Changes in occludin localization and structure during HR can be pharmacologically inhibited by pre-treating rats with the stable, BBB permeable molecule tempol. HR and/or oxidative stress are important components of several disease states (i.e., cardiac arrest, stroke, high altitude cerebral edema) which exhibit a breakdown in the BBB and subsequent neurotoxicity and cognitive impairment. It is possible that ROS produced during the HR phase of these pathological conditions

induces changes in occludin structure and localization, leading to a breakdown in the ability of the BBB to protect the CNS. Treatment of these conditions with antioxidant therapy may preserve the functional integrity of the BBB which may ultimately decrease the amount of CNS damage associated with several pathological conditions.

CHAPTER 4

**ROLE OF REACTIVE OXYGEN SPECIES IN BLOOD-BRAIN BARRIER DISRUPTION DURING
PERIPHERAL INFLAMMATORY PAIN**

4.1 Introduction

Inflammatory pain is caused by an insult to the integrity of tissues at a cellular level. The most common noxious stimuli are thermal, mechanical, or chemical in nature. Once tissue damage occurs, nociceptors on pain fibers near the site of injury are activated and consequently transmit the signal up the spinothalamic tract to the brain where pain is perceived.

The production of reactive oxygen species (ROS) is a well-established component of both pain and inflammation (Salvemini et al., 2006). Tissue injury causes release of intracellular ROS, which leads to phagocyte recruitment from the systemic circulation. These phagocytes may then release pro-inflammatory cytokines and up-regulate various enzymes (i.e., myeloperoxidase, NADPH oxidase) that contribute to production of more ROS (Bodamyali et al., 2000). NADPH oxidase generates the superoxide anion (O_2^-), which is a critical mediator of hyperalgesia, as shown by studies with the superoxide dismutase mimetic drug M40403 (Wang et al., 2004). In the λ -carrageenan model of inflammatory pain, inhibition of superoxide dismutase (SOD) or administration of peroxynitrite prior to λ -carrageenan paw injection was shown to exacerbate paw edema (Khattab, 2006). Furthermore, pre-treatment with the free radical scavenger tempol attenuates both paw edema and hyperalgesia, suggesting that ROS play a key role in the progression of pain/inflammation in the periphery (Khattab, 2006).

Our laboratory has previously shown biphasic disruption of the BBB in a peripheral inflammatory pain model induced by hindpaw injection of λ -carrageenan or

complete Freund's adjuvant (Huber et al., 2001, Huber et al., 2002; Brooks et al., 2005; Brooks et al., 2006). These changes are associated with an increase in paracellular permeability (i.e. – leak to the brain) of ^{14}C -sucrose, a substrate that does not typically cross the BBB (Bhattacharjee et al. 2001). Furthermore, we have shown that peripheral inflammatory pain alters expression of various transmembrane TJ proteins (i.e., claudin-3, claudin-5, occludin) as well as zona occluden-1 (ZO-1), which anchors both claudins and occludin to the actin cytoskeleton and is critical to maintenance of high transendothelial electrical resistance (TEER) at the BBB (Ronaldson et al., 2009). Nociceptive input, transforming growth factor β (TGF- β) signaling, and prostaglandin synthesis due to cyclooxygenase activity have all been reported to be involved in BBB disruption under peripheral inflammatory pain conditions (Campos et al., 2008, Ronaldson et al., 2009, Brooks et al., 2008). These observations underscore the critical importance of both peripheral inflammation and centrally mediated mechanisms in BBB changes/leak during peripheral inflammatory pain.

At BBB endothelial cell TJ complexes, occludin exists in lipid rafts as high molecular weight oligomeric assemblies that are stabilized, in part, by disulfide bonds (McCaffrey et al., 2007). The C-terminal region of occludin has been shown to dimerize, through disulfide bonding, in a redox-sensitive process (Walter et al., 2009a, Walter et al., 2009b). Our laboratory has previously shown that occludin oligomers are structurally altered under conditions of peripheral inflammatory pain (McCaffrey et al., 2008) and hypoxia/reoxygenation (McCaffrey et al., 2009). Using tempol, we recently

demonstrated that oxidative stress increases BBB permeability *in vivo* to sucrose and causes alterations to occludin's structure and distribution during hypoxia-reoxygenation, implying that ROS are involved in disruption of BBB functional integrity (Lochhead et al., 2010). These observations led us to explore the role of ROS in BBB disruption during peripheral inflammatory pain.

In the present study, we used the stable, BBB permeable, nitroxide tempol to scavenge intracellular and extracellular ROS to examine specific effects of ROS on BBB paracellular permeability to ^{14}C -sucrose (i.e. leak) using a well-established *in vivo* model of peripheral inflammatory pain (i.e., λ -carrageenan-induced inflammatory pain (CIP)). Additionally, we investigated if ROS could induce structural protein changes (i.e., modulation of disulfide bonds in occludin oligomeric assemblies) to lipid raft-associated occludin oligomers at the TJ. These observations will further elucidate the role of oxidative stress in BBB disruption during peripheral inflammatory pain and point to novel therapeutic strategies for treatment of pain/inflammation.

4.2 Experimental Procedures

Radioisotopes, reagents, and chemicals

[^{14}C]-sucrose (9.6 mCi/mmol) was purchased from American Radiolabeled Chemicals (St. Louis, MO). Tempol was purchased from Arcos Organics (Geel, Belgium). Ts-2 tissue solubilizer was purchased from Research Products International (Mt. Prospect, IL). Optiphase Supermix scintillation cocktail was purchased from Perkin Elmer (Shelton,

CT). EDTA-free Complete Protease Inhibitors were purchased from Roche (Indianapolis, IN). OptiPrep was purchased from Accurate Chemical (Westbury, NY). The Coomassie Plus Better Bradford Assay Kit was purchased from Thermo Scientific (Rockford, IL). C-terminal rabbit anti-occludin and rabbit anti-NF- κ B p50 subunit antibodies were purchased from Zymed (San Francisco, CA). Secondary antibodies for Western blotting were purchased from Amersham (Pittsburgh, PA). The NE-PER nuclear and cytoplasmic extraction reagents were purchased from Thermo Scientific (Rockford, IL). Western Lightning enhanced chemiluminescence reagent was purchased from Perkin Elmer (Shelton, CT). XT sample buffer, XT reducing agent and Criterion gels were purchased from Bio-rad (Hercules, CA). All other antibodies or reagents, unless noted, were purchased from Sigma-Aldrich (St. Louis, MO).

Animals and Treatment

All experimental protocols were approved by the Institutional Animal Care and Use Committee (IACUC) at the University of Arizona College of Medicine and conform to National Institutes of Health guidelines. Adult female Sprague-Dawley rats (Harlan; Indianapolis, IN) weighing 230-280 g were housed under standard 12:12-h light-dark conditions and provided food and water *ad libitum*. Rats received an intraperitoneal (i.p.) injection of 0.9% saline or the free radical scavenger tempol (200 mg/kg body weight) 10 min prior to receiving a 100 μ l subcutaneous (s.c.) injection of 3% λ -carrageenan (in 0.9% saline) or 0.9% saline in the plantar surface of the right hind paw. Animals were anesthetized with sodium pentobarbital (64.8 mg/kg, i.p.) 3 h after paw

injection and prepared for *in situ* brain perfusion, microvessel isolation, or histology.

In Situ Brain Perfusion

The *in situ* brain perfusion technique was adapted from previously published methods (Zlokovic et al, 1986; Takasato et al, 1984) and performed as previously described (Lochhead et al, 2010). Briefly, 3 h after hind paw injection, rats were anesthetized with sodium pentobarbital (64.8 mg/kg, i.p.) prior to infusion with the paracellular permeability marker ^{14}C -sucrose (MW=342). Once anesthetized, rats were heparinized (10,000 U/kg) and carotid arteries were isolated and cannulated with silicon tubing. The perfusion medium consisted of a mammalian Ringer solution [117 mM NaCl, 4.7 mM KCl, 0.8 mM $\text{MgSO}_4\cdot\text{H}_2\text{O}$, 24.9 mM NaHCO_3 , 1.2 mM KH_2PO_4 , 2.5 mM $\text{CaCl}_2\cdot 6\text{H}_2\text{O}$, 10 mM D -glucose, 39 g/l dextran (MW 70,000) and 1 g/l BSA, 0.055 g/l Evans Blue] which was continuously bubbled with 95% O_2 /5% CO_2 gas mix. The Ringer solution was filtered, warmed to 37°C, and de-bubbled before arterial infusion at 3.1 ml/min. Once both carotid arteries were cannulated, the paracellular permeability marker ^{14}C -sucrose was infused into the perfusate inflow at 0.5 ml/min for 10 min, followed by a 1 min washout containing Ringer with no radioactive tracer.

At the end of the perfusion, the rat was decapitated and the brain was removed. The meninges and choroid plexuses were removed and the brain was sectioned and placed into pre-weighed vials. After weighing the vials, 1 ml of tissue solubilizer was added to each vial and allowed to dissolve the tissue for 48 h at room temperature.

Once solubilization was complete, 100 μ l of 30% glacial acetic acid was added to each sample to quench chemiluminescence. Optiphase Supermix scintillation cocktail (2.5 ml) was then added to each sample. Triplicate samples of 100 μ l aliquots of the perfusion medium were treated in the same manner as the perfused brain samples. All samples were then measured for disintegrations per minute (dpm) (1450 LSC and Luminescence Counter, Perkin Elmer; Waltham MA). The ratio of the concentration of ^{14}C -sucrose in tissue (C_{brain} , in dpm/g) was compared to perfusate ($C_{\text{perfusate}}$, in dpm/ml) and expressed as a percent ratio (i.e. - $R_{\text{brain}} = (C_{\text{brain}}/C_{\text{perfusate}}) \times 100\%$).

HPLC analysis of ^{14}C -sucrose degradation

Samples of the ^{14}C -sucrose standard, perfusate inflow and perfusate outflow were collected and analyzed for sucrose degradation using HPLC. Samples were injected onto a HPLC C18 column and subjected to a 7.5%-9% acetonitrile gradient for 10 min to separate ^{14}C -sucrose from potential metabolites. Radioactive counts per minute (cpm) were recorded to ensure no sucrose degradation occurred throughout the course of the brain perfusion.

Paw Edema Measurements

Paw edema was measured using a plethysmometer (model 7141, Ugo Basile, Comerio-Varese, Italy). Edema was measured as the volume of electrolyte solution displaced by the hind paw. To ensure consistency between measurements, the ankles were marked prior to inserting the hind paw into the plethysmometer. The hind paw was inserted

into the plethysmometer up to the marked line and paw volume was recorded.

Measurements were taken for the injected paw and the contralateral paw. All measurements were taken in triplicate.

Thermal Hyperalgesia

Hyperalgesia was measured using the Hargreaves radiant heat method 3 h after hind paw injection (Hargreaves et al., 1988). Paw withdrawal latency was measured as time (s) taken to remove the hind paw from the heat source. Rats were habituated to the plexiglass boxes on an elevated glass table for 15 min prior to measurements.

Measurements were taken for the injected hind paw and the contralateral paw. All measurements were taken in triplicate with a 2-5 min recovery periods between measurements.

Microvessel enrichment and fractionation

Rats were anesthetized with sodium pentobarbital (64.8 mg/kg) 3 h after paw injection.

They were then decapitated and the brains were harvested and placed in 4 ml of microvessel isolation buffer A [103 mM NaCl, 4.7 mM KCl, 2.5 mM CaCl₂, 1.2 mM KH₂PO₄, 1.2 mM MgSO₄, 15 mM HEPES, 2.5 mM NaHCO₃, 10 mM D-glucose, 1 mM sodium pyruvate, pH 7.4]. The cerebellum, meninges and choroid plexuses were removed and the cerebral hemispheres were then homogenized in 30 ml of microvessel isolation buffer B [103 mM NaCl, 4.7 mM KCl, 2.5 mM CaCl₂, 1.2 mM KH₂PO₄, 1.2 mM MgSO₄, 15 mM HEPES, 25 mM NaHCO₃, 10 mM glucose, 1 mM Na pyruvate, 1% dextran

MW 64 kD, pH 7.4] + protease inhibitors (Roche EDTA-free Complete Protease Inhibitor, 2 mmol/L PMSF, 1 mmol/L Na_3VO_4 , 1 mmol/L NaF and 1 mmol/L sodium pyrophosphate). The homogenates were then centrifuged at 5800g for 10 min at 4° C in ice-cold buffer A with 26% dextran. The supernatant was suctioned off and the pellets were centrifuged a second time at 5800g for 10 min at 4° C in buffer A with 26% dextran. Pellets were resuspended in buffer A with protease inhibitors then passed through a 100 μm filter. The filtrate was then passed through a 40 μm filter. The microvessels remaining on the filter were collected in buffer A and centrifuged at 1500g for 10 min. The pellet was then resuspended in 4 ml of buffer C [20 mM Tris-HCl, 250 mM sucrose, 1 mM CaCl_2 , 1mM MgCl_2 , pH 7.8] with protease inhibitors and drawn 20X through a 21 G needle. The protein concentration of each sample was then determined using the Coomassie Plus Better Bradford Assay Kit. Equal volumes amounts of microvessel homogenates (containing equal amounts of protein) were then mixed with 50% OptiPrep in buffer C. This suspension was layered beneath a discontinuous 0/5/10/15/20% Optiprep gradient (prepared in buffer C without ions) then centrifuged for 90 min at 52,000g at 4°C. One ml fractions were collected from the top of the gradient. Numerous aliquots of each fraction were stored at -20° C until later use.

Western Blot Analysis of Occludin Oligomeric Assemblies

Equal protein aliquots of each fraction were added to 4X XT sample buffer with or without XT reducing agent containing tris(2-carboxy-ethyl)phosphine hydrochloride (TCEP). Each fraction was then incubated at 70° C for 10 min before undergoing SDS-

PAGE on 10% Bis-Tris Criterion gels. Gels (reducing and non-reducing, for each treatment condition) were then transferred to PVDF membranes, blocked in 5% milk, and incubated overnight in 1° antibody (1:1000) with 1% milk. Blots were then washed, incubated in HRP-conjugated 2° antibody and detected using enhanced chemiluminescence reagent. The membranes were stained for total protein with Coomassie and the optical density (OD) of each band was normalized to the total protein in the lane according to previously published methods (Aldridge et al., 2008). Densitometry was performed using ImageJ software (Wayne Rasband, Research Services Branch, National Institutes of Mental Health, Bethesda, MD).

NF- κ B Nuclear Expression

Microvessels were isolated as above and nuclear and cytoplasmic extracts were prepared using NE-PER nuclear and cytoplasmic extraction reagents following the manufacturer's instructions. Equal amounts of protein from nuclear fractions were electrophoresed on 10% Bis-Tris gels and transferred to a PVDF membrane. Membranes were blocked in 5% milk and incubated in primary anti-NF- κ B p50 subunit antibody. Densitometry was performed using Image J software and the OD was normalized to the total protein in each lane as described above for occludin.

Statistical Analysis

SigmaPlot software was used to perform statistical analysis. Statistical significance was determined using one-way ANOVA, followed by Bonferroni's t-test. Data are presented

as means \pm SE. A value of $P < 0.05$ was considered statistically significant.

4.3 Results

Paw Edema and Thermal Hyperalgesia Measurements

Previous studies have demonstrated that the antioxidant tempol modulates carrageenan-induced paw edema and thermal hyperalgesia in rats (Khattab 2006). After paw injection (3h), λ -carrageenan induced a significant increase in paw edema and thermal hyperalgesia ($P < 0.001$). Tempol significantly decreased CIP induced paw edema and sensitivity to an infrared heat source (Figure 4.1). These data indicate that ROS are involved in both the inflammatory response and the animal's behavioral response to CIP.

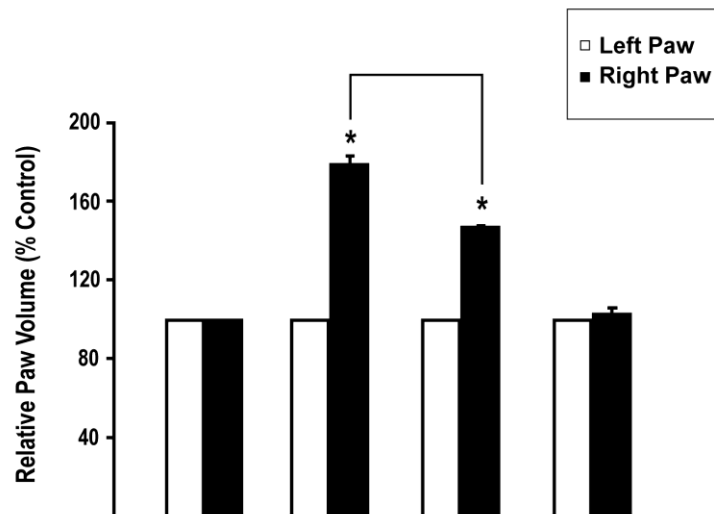
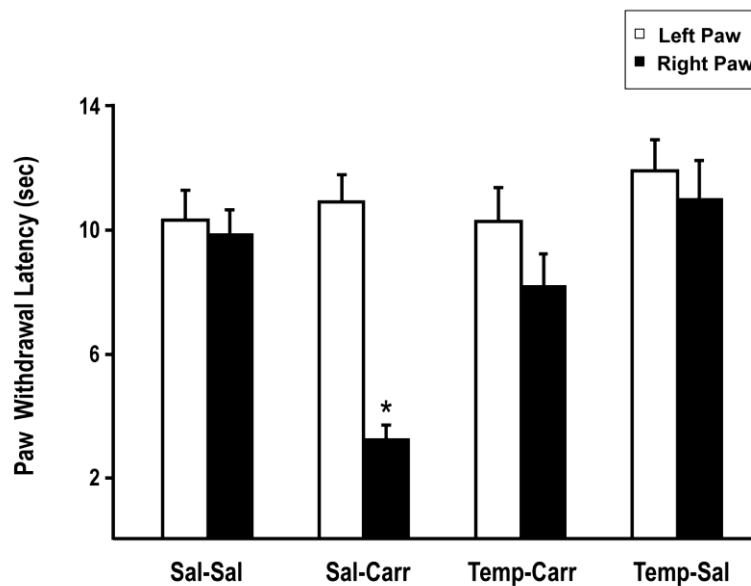
A**B**

Figure 4.1 Effect of CIP and tempol on paw edema and thermal hyperalgesia. **(A)** Edema formation in the injected paw (right) and the contralateral paw (left). Rats were given a i.p. injection of saline or tempol 10 min before paw injection of saline or 3% λ -carrageenan. Measurements were taken 3 h after paw injection. Results are expressed as mean \pm s.e. of 9 animals per treatment group. $P < 0.001$. **(B)** Paw withdrawal latency of the injected paw (right) and the contralateral paw (left) in rats given an i.p. injection of saline or tempol 10 min before paw injection of saline or 3% λ -carrageenan. Measurements were taken at 37°C 3 h after paw injection. Results are expressed as mean \pm s.e. of 6 animals per treatment group. $P < 0.001$

NF- κ B Nuclear Expression

NF- κ B is a redox-sensitive transcription factor which is present in the cytoplasm in an inactive state under physiological conditions and is one of the earliest responders to cellular stress (Sen and Smale, 2010). Once activated, NF- κ B translocates to the nucleus where it participates in gene transcription. NF- κ B has previously been shown to be activated by carrageenan-induced pleurisy and this activation was reduced by tempol (Cuzzocrea et al., 2004). We measured NF- κ B nuclear expression in enriched brain microvessel preparations to confirm cellular stress at the BBB due to carrageenan paw injection (Figure 4.2). We found carrageenan induced a significant increase (2.6-fold) in nuclear NF- κ B expression ($P < 0.05$) vs. saline control. Tempol significantly attenuated this increase (1.9-fold), suggesting ROS production is involved in carrageenan-induced nuclear NF- κ B expression at the BBB.

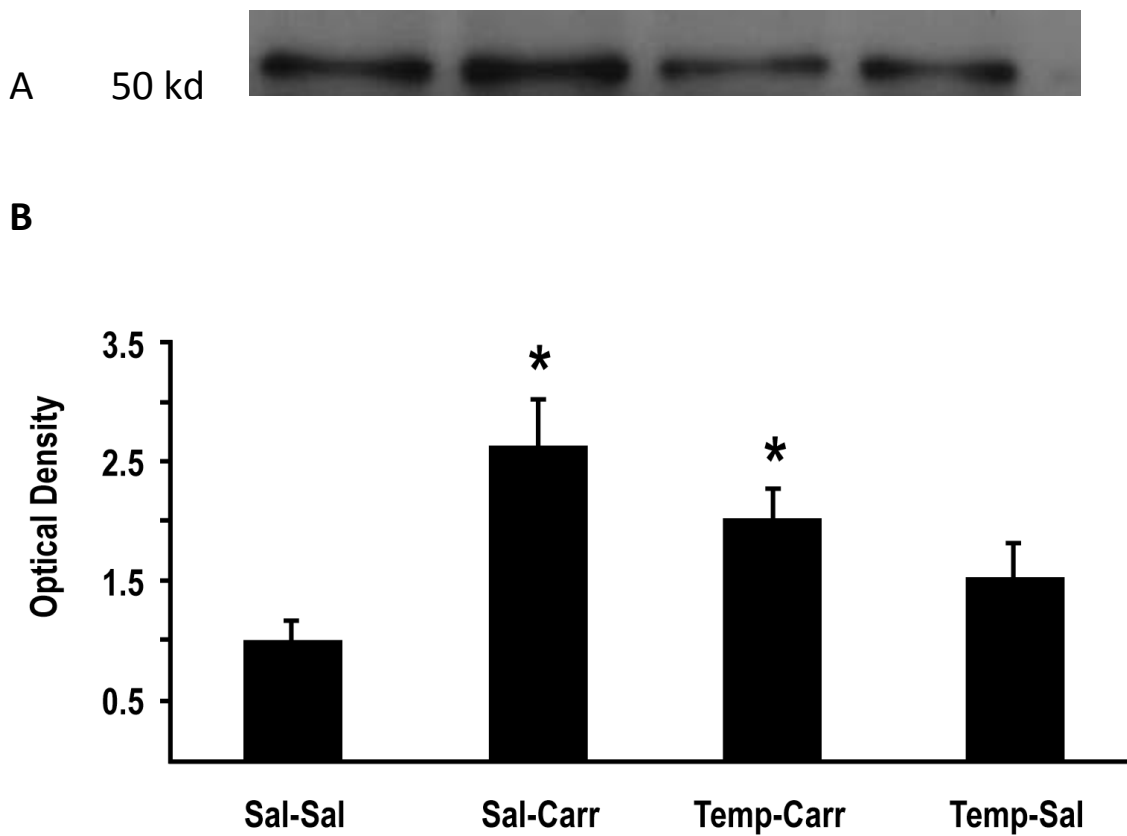


Figure 4.2 Nuclear Expression of NF- κ B. Rats were given an i.p. injection of saline or tempol 10 min before paw injection of saline or 3% λ -carrageenan. Representative Western blot of NF- κ B p50 subunit in nuclear extracts of brain microvessels (A). OD of the p50 subunit normalized to total protein (B). * $P < 0.01$. $P < 0.05$ vs. sal-sal and sal-carr. $N = 3-4$ rats per group.

BBB Permeability to ¹⁴C-sucrose

We investigated if oxidative stress was involved in regulating BBB paracellular permeability to ¹⁴C-sucrose during peripheral inflammatory pain using the *in situ* brain perfusion technique. In control animals, the Rbr was $1.67\% \pm 0.16\%$ (Figure 4.3). Hind paw injection of λ -carrageenan significantly increased the Rbr to $2.65\% \pm .21\%$ ($P < 0.05$), suggesting that peripheral inflammatory pain was associated with an increase in BBB paracellular permeability. Animals administered tempol before CIP had Rbr values of $2.08\% \pm 0.21\%$, a statistically significant decrease ($P < 0.05$) in Rbr compared to animals administered saline prior to CIP. This suggests oxidative stress was associated with the increase in BBB permeability during peripheral inflammatory pain. As an additional control, animals administered tempol before paw induction with saline had Rbr values of $1.51\% \pm 0.14\%$. HPLC analysis of the perfusate and the outflow was conducted to ensure the sucrose remained intact throughout the entire experiment. No degradation of radiolabeled sucrose was demonstrated by HPLC analysis (data not shown).

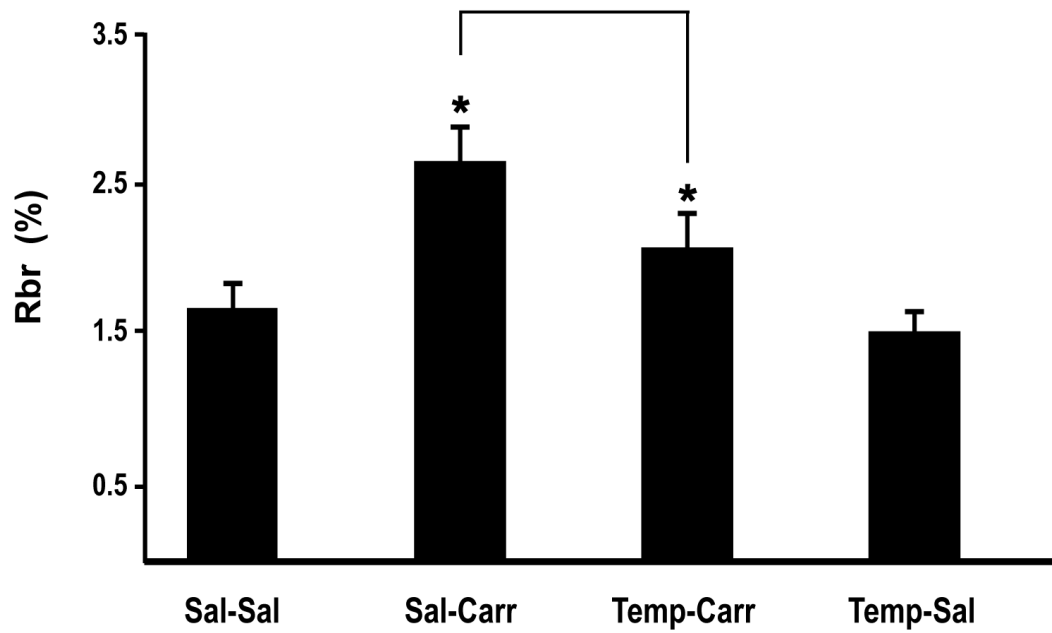


Figure 4.3 Effect of CIP and tempol on BBB permeability to ^{14}C -sucrose. Rats were given an i.p. injection of saline or tempol 10 min before paw injection of saline or 3% λ -Carrageenan. 3 h later, rats were anesthetized and subjected to in situ brain perfusion for 20 min with ^{14}C -sucrose. The amount of radioactivity in the brain vs. the perfusate was expressed as Rbr%. N = 6 rats per treatment group. P<0.05.

Western blot analysis of TJ occludin oligomers

Enriched microvessel preparations were subjected to density gradient subcellular fractionation to analyze TJ-associated plasma membrane lipid raft domains (fractions 7 and 8) containing oligomeric assemblies of occludin (McCaffrey et al., 2007). Equal protein aliquots of fractions 7 and 8 were examined by SDS PAGE/Western blot analysis under non-reducing and reducing conditions in order to identify changes in occludin oligomeric integrity due to disulfide-bond reduction. Figure 4.4A shows the banding pattern of occludin under non-reducing and reducing conditions in fractions 7 and 8 in control animals. Under non-reducing conditions, occludin is visualized almost exclusively as a single high molecular weight oligomer in these fractions. Upon exposure to the hydrophilic reducing agent TCEP, TJ-associated occludin is detected as a doublet, with the lower band representing a reduced oligomeric isoform. A greater amount of the reduced oligomeric isoform of occludin is present in the higher density fraction 8, which contains occludin oligomers that are not as tightly-packed and therefore more accessible to a hydrophilic reducing agent. Figure 4.4B shows representative Western blots of occludin oligomers electrophoresed under non-reducing and reducing conditions in all treatment groups. Given that the appearance of the reduced occludin oligomeric isoform is indicative of disulfide-bond reduction, relative changes in the measured OD of this band (under non-reducing conditions) were used to compare the effects of different treatments on occludin oligomeric integrity (Figure 4.4C). Samples prepared from animals treated with carrageenan revealed, under non-reducing

conditions only, significant increases in OD of the reduced oligomeric isoform, showing that inflammatory pain promotes cleavage of disulfide bonds within occludin oligomeric assemblies at the TJ. Tempol significantly decreased the OD of the reduced oligomeric occludin isoform, providing evidence that ROS did in fact induce disulfide bond breakage of occludin oligomers during inflammatory pain. As protein complexes with a structural role, alterations in disulfide bonding of occludin oligomeric assemblies may lead to changes in the functional integrity of the TJ at the BBB. The OD of occludin oligomers electrophoresed under non-reducing conditions in the saline-carrageenan treated group was significantly increased compared to the other treatment groups (P=0.003 vs. saline-saline, P=0.019 vs. tempol-carrageenan, P=0.015 vs. tempol-saline).

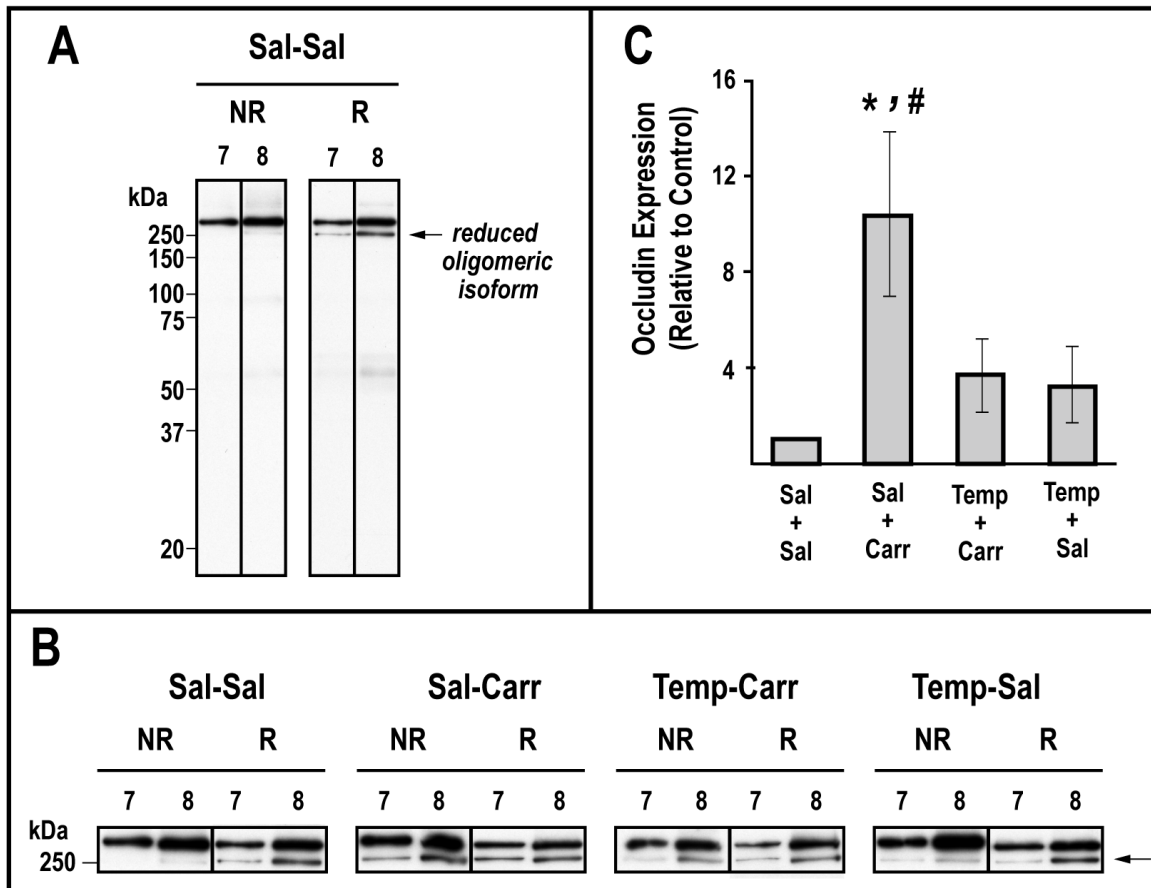


Figure 4.4 Effect of CIP and tempol on occludin oligomers. Rats were given an i.p. injection of saline or tempol 10 min before paw injection of saline or 3% λ -carrageenan. The banding pattern of occludin in non-reduced and reduced conditions in TJ fractions 7 and 8 in control animals is shown (A). Representative bands of TJ associated occludin oligomers under non-reducing and reducing conditions in all treatment groups (B). Optical density of the reduced TJ occludin oligomeric isoform (C). * $P < 0.005$ vs. saline-saline, # $P < 0.05$ vs. tempol-carrageenan and tempol-saline. $N = 3$ separate experiments with 3 animals pooled in each treatment group per experiment.

4.4 Discussion

The BBB is critical for maintaining CNS homeostasis. Disruption of the BBB's functional integrity is associated with numerous CNS disease states (Zlokovic, 2008). Our laboratory has previously demonstrated that BBB disruption (i.e. leak) is associated with acute peripheral inflammatory pain (Ronaldson et al., 2009, Brooks et al., 2008, Campos et al., 2008). These changes include altered expression of TJ proteins that form complexes between endothelial cells which greatly restrict paracellular permeability of substances from the blood into the brain. We have previously shown that oxidative stress is involved in BBB disruption in a rat model of hypoxia/reoxygenation (Lochhead et al., 2010). Additionally, oxidative stress is a central component of the inflammatory pain response (Little et al., 2010). These observations led us to examine the role of oxidative stress in BBB disruption during peripheral inflammatory pain using the free radical scavenger tempol.

We administered tempol to rats before inducing inflammatory pain by injecting their right hind paw with a solution of 3% λ -carrageenan (CIP). We found CIP increases paw edema and thermal hyperalgesia; however, tempol significantly reduced paw edema and hyperalgesia. This suggests ROS are involved in both inflammation and nociceptive signaling. The superoxide anion and peroxynitrite have previously been identified as mediators of paw edema and thermal hyperalgesia during inflammatory pain and are likely to contribute to these effects in this model (Khattab 2006, Wang et

al., 2004).

We found that hind-paw injection of λ -carrageenan increased expression of NF- κ B p50 subunit in the nucleus of brain microvessels. NF- κ B is a redox-sensitive transcription factor which translocates to the nucleus under conditions of cellular stress to activate genes involved in the inflammatory response (Camandola and Mattson, 2007). It has previously been shown that tempol reduces NF- κ B activation in the lung in carrageenan-induced pleurisy (Cuzzocrea et al., 2004). This is the first study to show that tempol inhibits NF- κ B activation in brain microvessels, indicating a role for ROS production in NF- κ B activation at the BBB during peripheral inflammatory pain.

We examined tempol's effects on BBB permeability using the well established *in situ* brain perfusion technique. This technique has advantages over other methods used to study the BBB because it avoids confounding variables associated with changes in peripheral blood flow, metabolism, and clearance. We measured BBB paracellular permeability to ^{14}C -sucrose, which shows very low diffusion across the BBB under control physiological conditions (Bhattacharjee, 2001). Peripheral inflammatory pain caused a significant increase in BBB paracellular permeability to ^{14}C -sucrose. In rats administered tempol, the increase in BBB permeability due to CIP was significantly decreased. This support our hypothesis and suggests that ROS produced during peripheral inflammatory pain are involved in disrupting the BBB's functional integrity and hence paracellular permeability.

The TJs are primarily responsible for maintaining low paracellular permeability across the brain capillary endothelium at the BBB. Occludin is one of the major components of the TJ (Feldman, 2005). At the BBB TJ, occludin exists in lipid rafts almost exclusively as high molecular weight (> 250 kD) oligomeric assemblies (McCaffrey et al., 2007). Using a newly developed, detergent-free, density gradient centrifugation and subcellular fractionation of enriched brain microvessel preparations, we have previously observed structural alterations in occludin oligomeric assemblies at the TJ during CIP and hypoxia/reoxygenation (McCaffrey et al., 2008; McCaffrey et al., 2009). Disruption of occludin oligomeric assemblies during hypoxia/reoxygenation was attenuated with tempol (Lochhead et al., 2010). These observations led us to examine tempol's effects on occludin oligomers at the TJ during peripheral inflammatory pain. CIP induced no changes in the relative expression of occludin oligomers when the TJ samples are subjected to SDS PAGE and Western blot analysis under standard reducing conditions. Interestingly, when the same samples are subjected to SDS PAGE under non-reducing conditions, the optical density (OD) of a lower molecular weight, reduced oligomeric isoform of occludin is significantly increased by peripheral inflammatory pain. This suggests that CIP causes cleavage of disulfide bonds in occludin oligomeric assemblies. It has been suggested that the C-terminus of occludin is involved in oligomerization in a redox-sensitive manner through the formation of disulfide bonds (Walter et al., 2009a, Walter et al., 2009b). Conformational changes in occludin oligomers at the TJ of the BBB via disulfide bond cleavage may lead to an increase in paracellular permeability/leak. In

animals administered tempol, the increase in the OD of the reduced occludin oligomeric isoform at the TJ is significantly attenuated. These data are the first to suggest that ROS are involved in a re-establishment of the integrity of the TJ occludin oligomeric conformation that occurs during peripheral inflammatory pain and a reversal of BBB disruption due to CIP.

In summary, these experiments demonstrate, for the first time, involvement of ROS induced oxidative stress in BBB disruption during peripheral inflammatory pain insult. Our data suggest this process may be due to cleavage of disulfide bonds in the critical TJ protein occludin at the BBB. Compromised BBB functional integrity can lead to very serious and adverse consequences in the CNS due to an increase in neurotoxic substances and may also affect therapeutic drug delivery to the brain during pain/inflammation. These observations indicate that antioxidant capacity may influence one's response to a painful/inflammatory stimulus and suggest that free radical scavengers may be influence a patient's response during the treatment of pain/inflammation to maintain the intact nature necessary to the integrity of the BBB.

CHAPTER 5

SUMMARY AND CONCLUSIONS

The BBB allows the CNS to tightly regulate its environment so proper neuronal function may occur. Once thought to be a static structure, research over the past several decades has revealed the BBB to be dynamic. The functional integrity of the BBB is compromised in many disease states affecting the CNS. Most of these diseases exhibit oxidative stress as a component. Oxidative stress (i.e.- increased ROS)has previously been shown to increase BBB leak, but no studies have examined the effect of ROS production on the oligomeric assemblies of the TJ protein occludin *in vivo*. This dissertation demonstrates that oxidative stress disrupts the functional integrity of the BBB by inducing alterations in the TJ protein occludin.

In chapter 3 we investigated the involvement of ROS on BBB integrity during an acute (6% O₂, 1 h) hypoxic insult followed by reoxygenation (room air, 20 min). The stable nitroxide tempol was used as a pharmacological tool to scavenge both intracellular and extracellular ROS. We showed that HR induces translocation of the oxygen-sensitive transcription factor Hif-1 α from the cytoplasm to the nucleus to demonstrate that the brain microvessels were subjected to hypoxia. In addition, HR induced up-regulation of the cellular stress marker HSP-70 in brain microvessels. This effect was inhibited by tempol. *In situ* brain perfusion determined HR induced a significant increase to BBB permeability to ¹⁴C-sucrose, a marker of paracellular permeability. Confocal microscopy revealed that ROS cause an increase in punctuate staining of occludin in brain microvessels, suggesting the localization of occludin is affected by HR. We used density gradient subcellular fractionation and Western blot

analysis to examine the effects of ROS on lipid-raft associated occludin oligomeric assemblies at the BBB TJ. Reduced samples of all treatment groups showed no change in OD, indicating occludin expression did not change due to HR. In contrast, non-reduced samples showed a significantly greater occludin OD following HR. This suggests structural alterations of occludin oligomeric assemblies allow the antibody greater access to the antigen following HR, possibly due to reduction of disulfide bonds which are important in stabilizing occludin oligomeric assemblies. Tempol attenuated the increased OD of non-reduced occludin, suggesting that ROS are involved in structural rearrangements of occludin oligomeric assemblies at the TJ.

In chapter 4, we investigated the involvement of ROS on BBB integrity during peripheral inflammatory pain. We injected λ -carrageenan into the hind paw of rats with or without tempol pre-treatment. We found tempol attenuates the paw edema and thermal hyperalgesia associated with carrageenan injection. This indicates ROS are involved in nociception and the inflammatory response. We also found tempol attenuates NF- κ B nuclear expression in brain microvessels, suggesting ROS are involved in the BBB's stress response to peripheral inflammatory pain. Tempol also reduced BBB permeability to 14 C-sucrose during peripheral inflammatory pain, suggesting involvement of ROS in BBB disruption following carrageenan injection. We employed density gradient subcellular fractionation of brain microvessels and Western blot analysis to show there are no differences in occludin expression between treatment groups in reduced samples. The non-reduced samples, however, showed a prominent

band of occludin with a molecular weight corresponding to a reduced occludin oligomeric isoform in carrageenan treated rats. This effect was attenuated by tempol, suggesting ROS produced during peripheral inflammatory pain reduce disulfide bonds of occludin oligomeric assemblies.

Taken together, these studies show for the first time oxidative stress can affect the oligomeric assemblies of the TJ protein occludin and lead to an increase in BBB paracellular permeability (i.e. – leak). We demonstrate this in two different animal models of disease states (hypoxia and pain) closely associated with the production of ROS. Tempol completely inhibited the increase in BBB permeability during HR, but only partially inhibited the BBB permeability increase during peripheral inflammatory pain. ROS increased changes in the percentage of microvessels exhibiting punctate staining of occludin during HR, but this effect was not seen during peripheral inflammatory pain. These differences may be due to the origin of ROS in the two disparate animal models. During HR, most of the ROS are thought to be produced primarily in the mitochondria of hypoxic cells. During inflammatory pain, ROS are thought to be produced primarily by phagocytes and pro-inflammatory signaling pathways. These differences may affect the types of ROS produced, the localization of ROS, or both. Alternately, differences in the time point examined in the two models may explain the discrepancies as well. Our HR treatment was 1 h 20 min while our inflammatory pain treatment was 3 h. Observations in the HR model not seen in the carrageenan model may be due to the earlier time point studied. This would suggest ROS play a prominent role in BBB disruption during the early

phase of ROS production, but other mechanisms may be more important at later time points.

Future studies should address the role of ROS in PKC or NOS expression and/or activation, which have been linked to BBB permeability changes in the HR model (Mark et al., 2004; Fleegal et al., 2005; Willis et al., 2008). In the inflammatory pain model, changes in TGF- β and COX expression and signaling have been linked to BBB disruption (Brooks et al., 2008; Ronaldson et al., 2009). Effects of tempol on TGF- β signaling and COX activity should be examined. Additionally, both HR and inflammatory pain cause BBB disruption in a biphasic manner (Witt et al. 2008; Huber et al., 2002). The use of antioxidants to preserve BBB functional integrity at later time points should also be studied.

We conclude from these studies that ROS impair BBB functional integrity. Hypoxia and/or inflammation are components of many disease states which ultimately compromise CNS function. BBB disruption may allow neurotoxic substances in the blood to leak into the brain. Over time this may cause or contribute to the cognitive impairment and/or neurodegeneration that is often observed in patients experiencing hypoxia and/or inflammation. Delivery of therapeutics to the brain is also likely to be affected by a compromise in BBB integrity. Drug concentrations in the CNS could potentially reach unsafe levels if the BBB's ability to restrict paracellular diffusion is impaired (Hau et al., 2004; Seelbach et al., 2007; Ronaldson et al., 2010). Our data suggests antioxidant therapy may be beneficial in preserving the BBB's functional

integrity during an insult involving oxidative stress.

REFERENCES

- Annunziata, P., C. Cioni, et al. (1998). "HIV-1 gp120 increases the permeability of rat brain endothelium cultures by a mechanism involving substance P." *Aids* 12(18): 2377-85.
- Arese, M., C. Ferrandi, et al. (2001). "HIV-1 Tat protein stimulates in vivo vascular permeability and lymphomononuclear cell recruitment." *J Immunol* 166(2): 1380-8.
- Augusto, O., D. F. Trindade, et al. (2008). "Cyclic nitroxides inhibit the toxicity of nitric oxide-derived oxidants: mechanisms and implications." *An Acad Bras Cienc* 80(1): 179-89.
- Balda, M. S., C. Flores-Maldonado, et al. (2000). "Multiple domains of occludin are involved in the regulation of paracellular permeability." *J Cell Biochem* 78(1): 85-96.
- Bauer, H., J. Zweimueller-Mayer, et al. "The dual role of zonula occludens (ZO) proteins." *J Biomed Biotechnol* 2010: 402593.
- Bell, R. D. and B. V. Zlokovic (2009). "Neurovascular mechanisms and blood-brain barrier disorder in Alzheimer's disease." *Acta Neuropathol* 118(1): 103-13.
- Bergamini, C. M., S. Gambetti, et al. (2004). "Oxygen, reactive oxygen species and tissue damage." *Curr Pharm Des* 10(14): 1611-26.
- Bergendi, L., L. Benes, et al. (1999). "Chemistry, physiology and pathology of free radicals." *Life Sci* 65(18-19): 1865-74.
- Boven, L. A., J. Middel, et al. (2000). "Monocyte infiltration is highly associated with loss of the tight junction protein zonula occludens in HIV-1-associated dementia." *Neuropathol Appl Neurobiol* 26(4): 356-60.
- Bowman, G. L., J. A. Kaye, et al. (2007). "Blood-brain barrier impairment in Alzheimer disease: stability and functional significance." *Neurology* 68(21): 1809-14.
- Brightman, M. W. and T. S. Reese (1969). "Junctions between intimately apposed cell membranes in the vertebrate brain." *J Cell Biol* 40(3): 648-77.
- Brooks, T. A., B. T. Hawkins, et al. (2005). "Chronic inflammatory pain leads to increased blood-brain barrier permeability and tight junction protein alterations." *Am J Physiol Heart Circ Physiol* 289(2): H738-43.
- Brooks, T. A., N. Nametz, et al. (2008). "Diclofenac attenuates the regional effect of

- lambda-carrageenan on blood-brain barrier function and cytoarchitecture." *J Pharmacol Exp Ther* 325(2): 665-73.
- Brooks, T. A., S. M. Ocheltree, et al. (2006). "Biphasic cytoarchitecture and functional changes in the BBB induced by chronic inflammatory pain." *Brain Res* 1120(1): 172-82.
- Brown, R. C. and T. P. Davis (2005). "Hypoxia/aglycemia alters expression of occludin and actin in brain endothelial cells." *Biochem Biophys Res Commun* 327(4): 1114-23.
- Butt, A. M., H. C. Jones, et al. (1990). "Electrical resistance across the blood-brain barrier in anaesthetized rats: a developmental study." *J Physiol* 429: 47-62.
- Campos, C. R., S. M. Ocheltree, et al. (2008). "Nociceptive inhibition prevents inflammatory pain induced changes in the blood-brain barrier." *Brain Res* 1221: 6-13.
- Carvey, P. M., B. Hendey, et al. (2009). "The blood-brain barrier in neurodegenerative disease: a rhetorical perspective." *J Neurochem* 111(2): 291-314.
- Caza, N., R. Taha, et al. (2008). "The effects of surgery and anesthesia on memory and cognition." *Prog Brain Res* 169: 409-22.
- Chen, W., R. Hartman, et al. (2009). "Matrix metalloproteinases inhibition provides neuroprotection against hypoxia-ischemia in the developing brain." *J Neurochem* 111(3): 726-36.
- Chen, Y., C. Merzdorf, et al. (1997). "COOH terminus of occludin is required for tight junction barrier function in early *Xenopus* embryos." *J Cell Biol* 138(4): 891-9.
- Crone, C. and S. P. Olesen (1982). "Electrical resistance of brain microvascular endothelium." *Brain Res* 241(1): 49-55.
- Cuzzocrea, S., M. C. McDonald, et al. (2000). "Effects of tempol, a membrane-permeable radical scavenger, in a gerbil model of brain injury." *Brain Res* 875(1-2): 96-106.
- Dallasta, L. M., L. A. Pizarov, et al. (1999). "Blood-brain barrier tight junction disruption in human immunodeficiency virus-1 encephalitis." *Am J Pathol* 155(6): 1915-27.
- Dauchy, S., F. Dutheil, et al. (2008). "ABC transporters, cytochromes P450 and their main transcription factors: expression at the human blood-brain barrier." *J Neurochem* 107(6): 1518-28.
- Deane, R., A. Sagare, et al. (2005). "IgG-assisted age-dependent clearance of Alzheimer's

- amyloid beta peptide by the blood-brain barrier neonatal Fc receptor." *J Neurosci* 25(50): 11495-503.
- Deane, R., Z. Wu, et al. (2004). "LRP/amyloid beta-peptide interaction mediates differential brain efflux of A β isoforms." *Neuron* 43(3): 333-44.
- Deng-Bryant, Y., I. N. Singh, et al. (2008). "Neuroprotective effects of tempol, a catalytic scavenger of peroxynitrite-derived free radicals, in a mouse traumatic brain injury model." *J Cereb Blood Flow Metab* 28(6): 1114-26.
- Di Virgilio, F. (2004). "New pathways for reactive oxygen species generation in inflammation and potential novel pharmacological targets." *Curr Pharm Des* 10(14): 1647-52.
- Dobbing J (1961) The blood-brain barrier. *Physiol. Rev* 41:130-88
- Dodelet-Devillers, A., R. Cayrol, et al. (2009). "Functions of lipid raft membrane microdomains at the blood-brain barrier." *J Mol Med* 87(8): 765-74.
- Donahue, J. E., S. L. Flaherty, et al. (2006). "RAGE, LRP-1, and amyloid-beta protein in Alzheimer's disease." *Acta Neuropathol* 112(4): 405-15.
- Dore-Duffy, P. (2008). "Pericytes: pluripotent cells of the blood brain barrier." *Curr Pharm Des* 14(16): 1581-93.
- Ehrlich P. 1885. Das Sauerstoffbedurfnis des Organismus.
- El-Ad, B. and P. Lavie (2005). "Effect of sleep apnea on cognition and mood." *Int Rev Psychiatry* 17(4): 277-82.
- Estrada, C., J. V. Bready, et al. (1990). "Astrocyte growth stimulation by a soluble factor produced by cerebral endothelial cells in vitro." *J Neuropathol Exp Neurol* 49(6): 539-49.
- Feldman, G. J., J. M. Mullin, et al. (2005). "Occludin: structure, function and regulation." *Adv Drug Deliv Rev* 57(6): 883-917.
- Fischer, S., M. Wobben, et al. (2002). "Hypoxia-induced hyperpermeability in brain microvessel endothelial cells involves VEGF-mediated changes in the expression of zonula occludens-1." *Microvasc Res* 63(1): 70-80.
- Fisher, M. (2009). "Pericyte signaling in the neurovascular unit." *Stroke* 40(3 Suppl): S13-5.
- Fleegal, M. A., S. Hom, et al. (2005). "Activation of PKC modulates blood-brain barrier endothelial cell permeability changes induced by hypoxia and posthypoxic

- reoxygenation." *Am J Physiol Heart Circ Physiol* 289(5): H2012-9.
- Forman, H. J., M. Maorino, et al. "Signaling functions of reactive oxygen species." *Biochemistry* 49(5): 835-42.
- Forster, C. (2008). "Tight junctions and the modulation of barrier function in disease." *Histochem Cell Biol* 130(1): 55-70.
- Furuse, M., T. Hirase, et al. (1993). "Occludin: a novel integral membrane protein localizing at tight junctions." *J Cell Biol* 123(6 Pt 2): 1777-88.
- Furuse, M., M. Itoh, et al. (1994). "Direct association of occludin with ZO-1 and its possible involvement in the localization of occludin at tight junctions." *J Cell Biol* 127(6 Pt 1): 1617-26.
- Furuse, M., H. Sasaki, et al. (1999). "Manner of interaction of heterogeneous claudin species within and between tight junction strands." *J Cell Biol* 147(4): 891-903.
- Giese, H., K. Mertsch, et al. (1995). "Effect of MK-801 and U83836E on a porcine brain capillary endothelial cell barrier during hypoxia." *Neurosci Lett* 191(3): 169-72.
- Guillemin, G. J. and B. J. Brew (2004). "Microglia, macrophages, perivascular macrophages, and pericytes: a review of function and identification." *J Leukoc Biol* 75(3): 388-97.
- Gumbiner, B., T. Lowenkopf, et al. (1991). "Identification of a 160-kDa polypeptide that binds to the tight junction protein ZO-1." *Proc Natl Acad Sci U S A* 88(8): 3460-4.
- Han H.S. and K. Suk (2005). "The function and integrity of the neurovascular unit rests upon the integration of the vascular and inflammatory cell systems. *Curr Neurovasc Res* 2:409-423.
- Hackett, P. H. (1999). "High altitude cerebral edema and acute mountain sickness. A pathophysiology update." *Adv Exp Med Biol* 474: 23-45.
- Haddad, J. J. and S. C. Land (2001). "A non-hypoxic, ROS-sensitive pathway mediates TNF-alpha-dependent regulation of HIF-1alpha." *FEBS Lett* 505(2): 269-74.
- Hamilton, N. B., D. Attwell, et al. "Pericyte-mediated regulation of capillary diameter: a component of neurovascular coupling in health and disease." *Front Neuroenergetics* 2.
- Haorah, J., D. Heilman, et al. (2005). "Ethanol-induced activation of myosin light chain kinase leads to dysfunction of tight junctions and blood-brain barrier compromise." *Alcohol Clin Exp Res* 29(6): 999-1009.

- Haorah, J., S. H. Ramirez, et al. (2007). "Oxidative stress activates protein tyrosine kinase and matrix metalloproteinases leading to blood-brain barrier dysfunction." *J Neurochem* 101(2): 566-76.
- Hardy, J. and D. J. Selkoe (2002). "The amyloid hypothesis of Alzheimer's disease: progress and problems on the road to therapeutics." *Science* 297(5580): 353-6.
- Hassel, B., E. G. Iversen, et al. (1994). "Neurotoxicity of albumin in vivo." *Neurosci Lett* 167(1-2): 29-32.
- Hawkins, B. T., T. J. Abbruscato, et al. (2004). "Nicotine increases in vivo blood-brain barrier permeability and alters cerebral microvascular tight junction protein distribution." *Brain Res* 1027(1-2): 48-58.
- Hiu, T., S. Nakagawa, et al. (2008). "Tissue plasminogen activator enhances the hypoxia/reoxygenation-induced impairment of the blood-brain barrier in a primary culture of rat brain endothelial cells." *Cell Mol Neurobiol* 28(8): 1139-46.
- Holman, D. W., R. S. Klein, et al. "The blood-brain barrier, chemokines and multiple sclerosis." *Biochim Biophys Acta*.
- Hom, S., M. A. Fleegal, et al. (2007). "Comparative changes in the blood-brain barrier and cerebral infarction of SHR and WKY rats." *Am J Physiol Regul Integr Comp Physiol* 292(5): R1881-92.
- Hopkins, R. O., S. D. Gale, et al. (2006). "Brain atrophy and cognitive impairment in survivors of Acute Respiratory Distress Syndrome." *Brain Inj* 20(3): 263-71.
- Huber, J. D., V. S. Hau, et al. (2002). "Blood-brain barrier tight junctions are altered during a 72-h exposure to lambda-carrageenan-induced inflammatory pain." *Am J Physiol Heart Circ Physiol* 283(4): H1531-7.
- Huber, J. D., K. A. Witt, et al. (2001). "Inflammatory pain alters blood-brain barrier permeability and tight junctional protein expression." *Am J Physiol Heart Circ Physiol* 280(3): H1241-8.
- Huber, J.D. (2008). "Diabetes, cognitive function, and the blood-brain barrier." *Curr Pharm Des* 2008;14(16):1594-600.
- Huelsken, J., R. Vogel, et al. (2000). "Requirement for beta-catenin in anterior-posterior axis formation in mice." *J Cell Biol* 148(3): 567-78.
- Inoko, A., M. Itoh, et al. (2003). "Expression and distribution of ZO-3, a tight junction MAGUK protein, in mouse tissues." *Genes Cells* 8(11): 837-45.
- Itoh, M., K. Morita, et al. (1999). "Characterization of ZO-2 as a MAGUK

- family member associated with tight as well as adherens junctions with a binding affinity to occludin and alpha catenin." *J Biol Chem* 274(9): 5981-6.
- Jacobson, K., O. G. Mouritsen, et al. (2007). "Lipid rafts: at a crossroad between cell biology and physics." *Nat Cell Biol* 9(1): 7-14.
- Janzer, R. C. and M. C. Raff (1987). "Astrocytes induce blood-brain barrier properties in endothelial cells." *Nature* 325(6101): 253-7.
- Jiang, H., A. S. Weyrich, et al. (2004). "Endothelial cell confluence regulates cyclooxygenase-2 and prostaglandin E2 production that modulate motility." *J Biol Chem* 279(53): 55905-13.
- Kahles, T., P. Luedike, et al. (2007). "NADPH oxidase plays a central role in blood-brain barrier damage in experimental stroke." *Stroke* 38(11): 3000-6.
- Kalaria, R. N. and C. Ballard (2001). "Stroke and cognition." *Curr Atheroscler Rep* 3(4): 334-9.
- Kamada, H., F. Yu, et al. (2007). "Influence of hyperglycemia on oxidative stress and matrix metalloproteinase-9 activation after focal cerebral ischemia/reperfusion in rats: relation to blood-brain barrier dysfunction." *Stroke* 38(3): 1044-9.
- Katsuno, T., K. Umeda, et al. (2008). "Deficiency of zonula occludens-1 causes embryonic lethal phenotype associated with defected yolk sac angiogenesis and apoptosis of embryonic cells." *Mol Biol Cell* 19(6): 2465-75.
- Kermode, A. G., A. J. Thompson, et al. (1990). "Breakdown of the blood-brain barrier precedes symptoms and other MRI signs of new lesions in multiple sclerosis. Pathogenetic and clinical implications." *Brain* 113 (Pt 5): 1477-89.
- Kim, G. W., Y. Gasche, et al. (2003). "Neurodegeneration in striatum induced by the mitochondrial toxin 3-nitropropionic acid: role of matrix metalloproteinase-9 in early blood-brain barrier disruption?" *J Neurosci* 23(25): 8733-42.
- Kim, G. W., A. Lewen, et al. (2001). "The cytosolic antioxidant, copper/zinc superoxide dismutase, attenuates blood-brain barrier disruption and oxidative cellular injury after photothrombotic cortical ischemia in mice." *Neuroscience* 105(4): 1007-18.
- Kimura, C., W. Cheng, et al. (2002). "Superoxide anion impairs contractility in cultured aortic smooth muscle cells." *Am J Physiol Heart Circ Physiol* 283(1): H382-90.
- Kimura, C., M. Oike, et al. (2000). "Hypoxia-induced alterations in Ca(2+) mobilization in brain microvascular endothelial cells." *Am J Physiol Heart Circ Physiol* 279(5): H2310-8.

- Kohen, R. and A. Nyska (2002). "Oxidation of biological systems: oxidative stress phenomena, antioxidants, redox reactions, and methods for their quantification." *Toxicol Pathol* 30(6): 620-50.
- Koto, T., K. Takubo, et al. (2007). "Hypoxia disrupts the barrier function of neural blood vessels through changes in the expression of claudin-5 in endothelial cells." *Am J Pathol* 170(4): 1389-97.
- Kowaltowski, A. J., N. C. de Souza-Pinto, et al. (2009). "Mitochondria and reactive oxygen species." *Free Radic Biol Med* 47(4): 333-43.
- Krizbai, I. A., H. Bauer, et al. (2005). "Effect of oxidative stress on the junctional proteins of cultured cerebral endothelial cells." *Cell Mol Neurobiol* 25(1): 129-39.
- Kuhlmann, C. R., R. Tamaki, et al. (2007). "Inhibition of the myosin light chain kinase prevents hypoxia-induced blood-brain barrier disruption." *J Neurochem* 102(2): 501-7.
- Kurzepa, J., H. Bartosik-Psujek, et al. (2005). "[Role of matrix metalloproteinases in the pathogenesis of multiple sclerosis]." *Neurol Neurochir Pol* 39(1): 63-7.
- Kwon, T. H., D. L. Chao, et al. (2003). "Tempol, a novel stable nitroxide, reduces brain damage and free radical production, after acute subdural hematoma in the rat." *J Neurotrauma* 20(4): 337-45.
- Laranjinha J. (2009). "Oxidative stress from the 1980's to Recent Update." Edited by Soares R. and C. Costa in *Oxidative stress, SInflammation, and Angiogenesis in the Metabolic Syndrome*. 21-32.
- Leckband, D. and S. Sivasankar (2000). "Mechanism of homophilic cadherin adhesion." *Curr Opin Cell Biol* 12(5): 587-92.
- Lehner C., R Gehwolf (2010). "Oxidative stress and blood-brain barrier dysfunction." *Antioxid Redox Signal* (in press).
- Lewandowsky M. (1900) Zur Lehre von der Cerebrospinalflüssigkeit. *Z klin Med* 40:480-494
- Lee, H. S., K. Namkoong, et al. (2004). "Hydrogen peroxide-induced alterations of tight junction proteins in bovine brain microvascular endothelial cells." *Microvasc Res* 68(3): 231-8.
- Li, C. and R. M. Jackson (2002). "Reactive species mechanisms of cellular hypoxia-reoxygenation injury." *Am J Physiol Cell Physiol* 282(2): C227-41.
- Lim, C., M. P. Alexander, et al. (2004). "The neurological and cognitive sequelae of

- cardiac arrest." *Neurology* 63(10): 1774-8.
- Lippoldt, A., S. Liebner, et al. (2000). "Organization of choroid plexus epithelial and endothelial cell tight junctions and regulation of claudin-1, -2 and -5 expression by protein kinase C." *Neuroreport* 11(7): 1427-31.
- Liu, Y., X. P. Tang, et al. (2000). "Analysis of human immunodeficiency virus type 1 gp160 sequences from a patient with HIV dementia: evidence for monocyte trafficking into brain." *J Neurovirol* 6 Suppl 1: S70-81.
- Lochhead, J. J., G. McCaffrey, et al. "Oxidative stress increases blood-brain barrier permeability and induces alterations in occludin during hypoxia-reoxygenation." *J Cereb Blood Flow Metab* 30(9): 1625-36.
- Lok, J., P. Gupta, et al. (2007). "Cell-cell signaling in the neurovascular unit." *Neurochem Res* 32(12): 2032-45.
- Lu, D. Y., W. H. Yu, et al. (2009). "Hypoxia-induced matrix metalloproteinase-13 expression in astrocytes enhances permeability of brain endothelial cells." *J Cell Physiol* 220(1): 163-73.
- Mackic, J. B., M. Stins, et al. (1998). "Human blood-brain barrier receptors for Alzheimer's amyloid-beta 1-40. Asymmetrical binding, endocytosis, and transcytosis at the apical side of brain microvascular endothelial cell monolayer." *J Clin Invest* 102(4): 734-43.
- Mark, K. S. and T. P. Davis (2002). "Cerebral microvascular changes in permeability and tight junctions induced by hypoxia-reoxygenation." *Am J Physiol Heart Circ Physiol* 282(4): H1485-94.
- Martel, C. L., J. B. Mackic, et al. (1997). "Isoform-specific effects of apolipoproteins E2, E3, and E4 on cerebral capillary sequestration and blood-brain barrier transport of circulating Alzheimer's amyloid beta." *J Neurochem* 69(5): 1995-2004.
- Matter, K. and M. S. Balda (1998). "Biogenesis of tight junctions: the C-terminal domain of occludin mediates basolateral targeting." *J Cell Sci* 111 (Pt 4): 511-9.
- McCaffrey, G., M. J. Seelbach, et al. (2008). "Occludin oligomeric assembly at tight junctions of the blood-brain barrier is disrupted by peripheral inflammatory hyperalgesia." *J Neurochem* 106(6): 2395-409.
- McCaffrey, G., W. D. Staatz, et al. (2007). "Tight junctions contain oligomeric protein assembly critical for maintaining blood-brain barrier integrity in vivo." *J Neurochem*.

- McCaffrey, G., C. L. Willis, et al. (2009). "Occludin oligomeric assemblies at tight junctions of the blood-brain barrier are altered by hypoxia and reoxygenation stress." *J Neurochem* 110(1): 58-71.
- McCord, J. M. and I. Fridovich (1969). "Superoxide dismutase. An enzymic function for erythrocyte hemoglobin (hemocuprein)." *J Biol Chem* 244(22): 6049-55.
- McKelvey, T. G., M. E. Hollwarth, et al. (1988). "Mechanisms of conversion of xanthine dehydrogenase to xanthine oxidase in ischemic rat liver and kidney." *Am J Physiol* 254(5 Pt 1): G753-60.
- Medina, R., C. Rahner, et al. (2000). "Occludin localization at the tight junction requires the second extracellular loop." *J Membr Biol* 178(3): 235-47.
- Medinas, D. B., G. Cerchiaro, et al. (2007). "The carbonate radical and related oxidants derived from bicarbonate buffer." *IUBMB Life* 59(4-5): 255-62.
- Meier, B., H. H. Radeke, et al. (1989). "Human fibroblasts release reactive oxygen species in response to interleukin-1 or tumour necrosis factor-alpha." *Biochem J* 263(2): 539-45.
- Mertsch, K., I. Blasig, et al. (2001). "4-Hydroxynonenal impairs the permeability of an in vitro rat blood-brain barrier." *Neurosci Lett* 314(3): 135-8.
- Mi, H., H. Haeberle, et al. (2001). "Induction of astrocyte differentiation by endothelial cells." *J Neurosci* 21(5): 1538-47.
- Miller, D. S. "Regulation of P-glycoprotein and other ABC drug transporters at the blood-brain barrier." *Trends Pharmacol Sci* 31(6): 246-54.
- Misra, A., S. Ganesh, et al. (2003). "Drug delivery to the central nervous system: a review." *J Pharm Pharm Sci* 6(2): 252-73.
- Mohammed, H. O., S. R. Starkey, et al. (2008). "The role of dietary antioxidant insufficiency on the permeability of the blood-brain barrier." *J Neuropathol Exp Neurol* 67(12): 1187-93.
- Morita, K., M. Furuse, et al. (1999). "Claudin multigene family encoding four-transmembrane domain protein components of tight junction strands." *Proc Natl Acad Sci U S A* 96(2): 511-6.
- Nelson, C. W., E. P. Wei, et al. (1992). "Oxygen radicals in cerebral ischemia." *Am J Physiol* 263(5 Pt 2): H1356-62.
- Nelson, P.T., L.A. Soma, et al. (2002). "Microglia in diseases of the central nervous

- system." *Ann Med* 34(7-8):491-500.
- Neuwelt, E. A. (2004). "Mechanisms of disease: the blood-brain barrier." *Neurosurgery* 54(1): 131-40; discussion 141-2.
- Niessen, C. M. and C. J. Gottardi (2008). "Molecular components of the adherens junction." *Biochim Biophys Acta* 1778(3): 562-71.
- Nitta, T., M. Hata, et al. (2003). "Size-selective loosening of the blood-brain barrier in claudin-5-deficient mice." *J Cell Biol* 161(3): 653-60.
- Nicolazzo JA and K Katneni. "Drug transport across the blood-brain barrier and the impact of breast cancer resistant protein (ABCG2)." *Curr Top Med Chem* 9(2):130-47.
- Ohtsuki, S., S. Ito, et al. "Is P-glycoprotein involved in amyloid-beta elimination across the blood-brain barrier in Alzheimer's disease?" *Clin Pharmacol Ther* 88(4): 443-5.
- Pauling, L. (1979) "The discovery of the superoxide radical." *Trends in Biochemical Sciences*. 4:N270-N271.
- Peterson, D. A., S. L. Archer, et al. (1994). "Superoxide reduction of a disulfide: a model of intracellular redox modulation?" *Biochem Biophys Res Commun* 200(3): 1586-91.
- Petito, C. K. and K. S. Cash (1992). "Blood-brain barrier abnormalities in the acquired immunodeficiency syndrome: immunohistochemical localization of serum proteins in postmortem brain." *Ann Neurol* 32(5): 658-66.
- Plateel, M., M. P. Dehouck, et al. (1995). "Hypoxia increases the susceptibility to oxidant stress and the permeability of the blood-brain barrier endothelial cell monolayer." *J Neurochem* 65(5): 2138-45.
- Pun, P. B., J. Lu, et al. (2009). "Involvement of ROS in BBB dysfunction." *Free Radic Res* 43(4): 348-64.
- Rak, R., D. L. Chao, et al. (2000). "Neuroprotection by the stable nitroxide Tempol during reperfusion in a rat model of transient focal ischemia." *J Neurosurg* 92(4): 646-51.
- Ramirez, S. H., R. Potula, et al. (2009). "Methamphetamine disrupts blood-brain barrier function by induction of oxidative stress in brain endothelial cells." *J Cereb Blood*

- Flow Metab 29(12): 1933-45.
- Ramjeesingh, M., L. J. Huan, et al. (1999). "Novel method for evaluation of the oligomeric structure of membrane proteins." *Biochem J* 342 (Pt 1): 119-23.
- Ramsauer, M., D. Krause, et al. (2002). "Angiogenesis of the blood-brain barrier in vitro and the function of cerebral pericytes." *Faseb J* 16(10): 1274-6.
- Readnower, R. D., M. Chavko, et al. "Increase in blood-brain barrier permeability, oxidative stress, and activated microglia in a rat model of blast-induced traumatic brain injury." *J Neurosci Res* 88(16): 3530-9.
- Reese, T. S. and M. J. Karnovsky (1967). "Fine structural localization of a blood-brain barrier to exogenous peroxidase." *J Cell Biol* 34(1): 207-17.
- Rivest, S. (2009). "Regulation of innate immune responses in the brain." *Nat Rev Immunol* 9(6):429-39.
- Ronaldson, P.T. Babakhanian K., and R. Bendayan (2007) "Drug Transport in the Brain." Edited by G. You and M.E. Morris in *Molecular Characterization and role of Drug Disposition*:412-460.
- Ronaldson, P. T. and R. Bendayan (2008). "HIV-1 viral envelope glycoprotein gp120 produces oxidative stress and regulates the functional expression of multidrug resistance protein-1 (Mrp1) in glial cells." *J Neurochem* 106(3): 1298-313.
- Ronaldson, P. T., K. M. Demarco, et al. (2009). "Transforming growth factor-beta signaling alters substrate permeability and tight junction protein expression at the blood-brain barrier during inflammatory pain." *J Cereb Blood Flow Metab* 29(6): 1084-98.
- Ronaldson, P. T., J. D. Finch, et al. "Inflammatory Pain Signals an Increase in Functional Expression of Organic Anion Transporting Polypeptide 1a4 at the Blood-Brain Barrier." *J Pharmacol Exp Ther*.
- Rosenberg, G. A. and Y. Yang (2007). "Vasogenic edema due to tight junction disruption by matrix metalloproteinases in cerebral ischemia." *Neurosurg Focus* 22(5): E4.
- Rubin, L. L., D. E. Hall, et al. (1991). "A cell culture model of the blood-brain barrier." *J Cell Biol* 115(6): 1725-35.
- Saito, K., K. Takeshita, et al. (2003). "Two reaction sites of a spin label, TEMPOL (4-hydroxy-2,2,6,6-tetramethylpiperidine-N-oxyl), with hydroxyl radical." *J Pharm Sci* 92(2): 275-80.
- Salvemini, D., T. M. Doyle, et al. (2006). "Superoxide, peroxynitrite and

- oxidative/nitrative stress in inflammation." *Biochem Soc Trans* 34(Pt 5): 965-70.
- Sandoval, K. E. and K. A. Witt (2008). "Blood-brain barrier tight junction permeability and ischemic stroke." *Neurobiol Dis* 32(2): 200-19.
- Schoch, H. J., S. Fischer, et al. (2002). "Hypoxia-induced vascular endothelial growth factor expression causes vascular leakage in the brain." *Brain* 125(Pt 11): 2549-57.
- Schreibelt, G., G. Kooij, et al. (2007). "Reactive oxygen species alter brain endothelial tight junction dynamics via RhoA, PI3 kinase, and PKB signaling." *Faseb J* 21(13): 3666-76.
- Seelbach, M. J., T. A. Brooks, et al. (2007). "Peripheral inflammatory hyperalgesia modulates morphine delivery to the brain: a role for P-glycoprotein." *J Neurochem* 102(5): 1677-90.
- Sen, R. and S. T. Smale "Selectivity of the NF- κ B response." *Cold Spring Harb Perspect Biol* 2(4): a000257.
- Severson, E. A. and C. A. Parkos (2009). "Structural determinants of Junctional Adhesion Molecule A (JAM-A) function and mechanisms of intracellular signaling." *Curr Opin Cell Biol* 21(5): 701-7.
- Sharma, H. S., A. Miclescu, et al. "Cardiac arrest-induced regional blood-brain barrier breakdown, edema formation and brain pathology: a light and electron microscopic study on a new model for neurodegeneration and neuroprotection in porcine brain." *J Neural Transm.*
- Shibata, M., S. Yamada, et al. (2000). "Clearance of Alzheimer's amyloid-ss(1-40) peptide from brain by LDL receptor-related protein-1 at the blood-brain barrier." *J Clin Invest* 106(12): 1489-99.
- Smith, S. L., H. M. Scherch, et al. (1996). "Protective effects of tirilazad mesylate and metabolite U-89678 against blood-brain barrier damage after subarachnoid hemorrhage and lipid peroxidative neuronal injury." *J Neurosurg* 84(2): 229-33.
- Song, L., S. Ge, et al. (2007). "Caveolin-1 regulates expression of junction-associated proteins in brain microvascular endothelial cells." *Blood* 109(4): 1515-23.
- Sporer, B., U. Koedel, et al. (2000). "Human immunodeficiency virus type-1 Nef protein induces blood-brain barrier disruption in the rat: role of matrix metalloproteinase-9." *J Neuroimmunol* 102(2): 125-30.
- Stevenson, B. R., J. D. Siliciano, et al. (1986). "Identification of ZO-1: a high molecular

- weight polypeptide associated with the tight junction (zonula occludens) in a variety of epithelia." *J Cell Biol* 103(3): 755-66.
- Stewart, P. A. and M. J. Wiley (1981). "Developing nervous tissue induces formation of blood-brain barrier characteristics in invading endothelial cells: a study using quail--chick transplantation chimeras." *Dev Biol* 84(1): 183-92.
- Surh, Y. J., J. K. Kundu, et al. (2005). "Redox-sensitive transcription factors as prime targets for chemoprevention with anti-inflammatory and antioxidative phytochemicals." *J Nutr* 135(12 Suppl): 2993S-3001S.
- Tait, M. J., S. Saadoun, et al. (2008). "Water movements in the brain: role of aquaporins." *Trends Neurosci* 31(1): 37-43.
- Takasato, Y., S. I. Rapoport, et al. (1984). "An in situ brain perfusion technique to study cerebrovascular transport in the rat." *Am J Physiol* 247(3 Pt 2): H484-93.
- Takenaga, Y., N. Takagi, et al. (2009). "Inhibition of Src activity decreases tyrosine phosphorylation of occludin in brain capillaries and attenuates increase in permeability of the blood-brain barrier after transient focal cerebral ischemia." *J Cereb Blood Flow Metab* 29(6): 1099-108.
- Thannickal, V. J. and B. L. Fanburg (2000). "Reactive oxygen species in cell signaling." *Am J Physiol Lung Cell Mol Physiol* 279(6): L1005-28.
- Toborek, M., Y. W. Lee, et al. (2005). "Mechanisms of the blood-brain barrier disruption in HIV-1 infection." *Cell Mol Neurobiol* 25(1): 181-99.
- Tontsch, U. and H. C. Bauer (1991). "Glial cells and neurons induce blood-brain barrier related enzymes in cultured cerebral endothelial cells." *Brain Res* 539(2): 247-53.
- Tripathy, D. and P. Grammas (2009). "Acetaminophen inhibits neuronal inflammation and protects neurons from oxidative stress." *J Neuroinflammation* 6: 10.
- Ujiie, M., D. L. Dickstein, et al. (2003). "Blood-brain barrier permeability precedes senile plaque formation in an Alzheimer disease model." *Microcirculation* 10(6): 463-70.
- Umeda, K., T. Matsui, et al. (2004). "Establishment and characterization of cultured epithelial cells lacking expression of ZO-1." *J Biol Chem* 279(43): 44785-94.
- Vasioukhin, V., C. Bauer, et al. (2000). "Directed actin polymerization is the driving force for epithelial cell-cell adhesion." *Cell* 100(2): 209-19.
- Vogelgesang, S., I. Cascorbi, et al. (2002). "Deposition of Alzheimer's beta-amyloid is inversely correlated with P- glycoprotein expression in the brains of

- elderly non-demented humans." *Pharmacogenetics* 12(7): 535-41.
- Walter, J. K., V. Castro, et al. (2009). "Redox-sensitivity of the dimerization of occludin." *Cell Mol Life Sci* 66(22): 3655-62.
- Walter, J. K., C. Rueckert, et al. (2009). "The oligomerization of the coiled coil-domain of occludin is redox sensitive." *Ann N Y Acad Sci* 1165: 19-27.
- Wang, Z. Q., F. Porreca, et al. (2004). "A newly identified role for superoxide in inflammatory pain." *J Pharmacol Exp Ther* 309(3): 869-78.
- Willis, C. L., D. S. Meske, et al. "Protein kinase C activation modulates reversible increase in cortical blood-brain barrier permeability and tight junction protein expression during hypoxia and posthypoxic reoxygenation." *J Cereb Blood Flow Metab* 30(11): 1847-59.
- Witt, K. A., K. S. Mark, et al. (2003). "Effects of hypoxia-reoxygenation on rat blood-brain barrier permeability and tight junctional protein expression." *Am J Physiol Heart Circ Physiol* 285(6): H2820-31.
- Witt, K. A., K. S. Mark, et al. (2008). "Reoxygenation stress on blood-brain barrier paracellular permeability and edema in the rat." *Microvasc Res* 75(1): 91-6.
- Wong, C. H. and P. J. Crack (2008). "Modulation of neuro-inflammation and vascular response by oxidative stress following cerebral ischemia-reperfusion injury." *Curr Med Chem* 15(1): 1-14.
- Wong, V. and B. M. Gumbiner (1997). "A synthetic peptide corresponding to the extracellular domain of occludin perturbs the tight junction permeability barrier." *J Cell Biol* 136(2): 399-409.
- Xiong, H., D. Callaghan, et al. (2009). "ABCG2 is upregulated in Alzheimer's brain with cerebral amyloid angiopathy and may act as a gatekeeper at the blood-brain barrier for A β (1-40) peptides." *J Neurosci* 29(17): 5463-75.
- Yamagata, K., M. Tagami, et al. (2004). "Hypoxia-induced changes in tight junction permeability of brain capillary endothelial cells are associated with IL-1 β and nitric oxide." *Neurobiol Dis* 17(3): 491-9.
- Zlokovic, B. V. (2008). "The blood-brain barrier in health and chronic neurodegenerative disorders." *Neuron* 57(2): 178-201.
- Zlokovic, B. V., D. J. Begley, et al. (1985). "Blood-brain barrier permeability to leucine-enkephalin, D-alanine²-D-leucine⁵-enkephalin and their N-terminal amino acid (tyrosine)." *Brain Res* 336(1): 125- 32.

Zlokovic, B. V., D. J. Begley, et al. (1986). "Measurement of solute transport across the blood-brain barrier in the perfused guinea pig brain: method and application to N-methyl-alpha-aminoisobutyric acid." *J Neurochem* 46(5): 1444-51.

Zollner, S., R. F. Haseloff, et al. (1997). "Nitroxides increase the detectable amount of nitric oxide released from endothelial cells." *J Biol Chem* 272(37): 23076-80.